# Characterization of Emissions from Small Scale Biomass Gasifier

A Thesis
SUBMITTED TO THE FACULTY OF
UNIVERSITY OF MINNESOTA
BY

Jaimie Emma Hamilton

IN PARTIAL FULFILLMENT OF THE REQUIREMENTS
FOR THE DEGREE OF
MASTER OF SCIENCE

*Dr. William Northrop*

November 2013

**Acknowledgements**

I would like to acknowledge the constant encouragement, guidance, and support from Dr. William Northrop throughout this project. Without his patience, knowledge and effort this work would not be in its current form. I would also like to thank Darrick Zarling for his help in the experimental setup, particularly in the early stages of the project. His experience and guidance was instrumental in the success of the project. I would also like to recognize the assistance from Win Watts, who helped immensely with the particulate matter studies. I would also like to thank Dr. David Kittleson and Dr. Jonathan Chaplin for their assistance throughout the project. I give my eternal gratitude to John Adams for his help during the experiments and for making everything just a little bit easier. His patience, knowledge, and skills were invaluable to this work. I would also like to thank all the members of the Center for Diesel Research for their assistance and guidance at various stages throughout the project. Finally, I thank my parents and sister for their encouragement, guidance and support, even when they didn't know what on earth I was talking about.

## Abstract

Gasification of biomass has the potential to address many issues related to both the world's energy future and greenhouse gas emissions. Gasification can be carried out in a variety of ways depending on the end-use application of the synthesis gas (syngas) or producer gas. Gasification can also use a variety of feedstocks. Gasifying agricultural waste to generate electricity or provide heating and cooling solutions has the potential to utilize waste products while providing necessary energy. Unfortunately, there are environmental and human health concerns related to the conversion of biomass to energy and the combustion of the bio-derived fuel, as well as efficiency concerns related to the technology.

In this study, The Power Pallet, a commercially available integrated gasification reactor, engine and generator was used to quantify the contaminants in the unfiltered producer gas, the filtered producer gas, and the engine exhaust and determine the engine's ability to reduce contaminants through filtration and combustion. The system was also tested to determine the effect of generator loading on operating conditions, emissions, and overall efficiency. The study used a fixed-bed downdraft modified Imbert reactor with a Kubota spark-ignited natural gas engine with a Mecc Alte 10kW generator. Organic solvent, gaseous and particulate matter emissions were characterized at three locations in the gasification system to determine the packed bed filter and engine's ability to reduce concentrations of contaminants.

Contaminants, such as benzene, toluene, ethylbenzene, and xylenes (BTEX) and

PM, in the gasifier system were cleaned up through the packed bed filter and through combustion in the engine. PM concentrations were approximately 70 mg/Nm$^3$ in the pre-filtered producer gas but concentrations were reduced 98-99% through the packed bed filter. PM concentrations did not change significantly during the combustion in the engine yet specific concentrations of PM were below federally mandated emissions limits for Tier 4 diesel engines. Combustible compound were 99% consumed in the engine and specific concentrations of carbon monoxide were below federally mandated levels from the engine's exhaust. Concentrations of BTEX compounds were reduced to a small degree in the packed bed filter and significantly reduced in the engine. Although concentrations of benzene in engine exhaust were greater than 10 ppm, operating the gasification system in a well-ventilated environment would ensure that the ambient air concentrations of BTEX compounds are below federal limits and protect human health and the environment from the hazards.

The efficiency of the reactor increased significantly with increasing electrical load because the reactor operates at constant temperature and the higher flow rates of biomass meant that the heat loss was a smaller portion of the work from the engine. The overall system efficiency increased with increasing electrical load and the efficiency of the engine was fairly steady over the small range of generator loads tested.

## Table of Contents

## List of Tables

## List of Figures

# 1. Introduction

## 1.1. Motivation:

As energy demands surge and new discoveries of conventional fossil fuels slow, it is increasingly important to address the world's energy demands with a renewable and sustainable energy source. Worldwide 1.4 billion people lack access to electricity, predominately in rural communities in the developing world. These communities traditionally rely on kerosene lanterns or candles for lighting, burning waste wood, charcoal, and manure for cooking and heating, dry-cell batteries for charging small electronics, and diesel generators for larger electrical needs (Buragohain et al., 2010). These energy sources can be scarce, expensive, and/or hazardous. Renewable energy has the potential to alleviate many of the human health and environmental hazards associated with conventional rural energy sources, while reducing the costs associated with energy generation and improving the quality of life for people in the communities. Increased access to electricity and reliable heating and cooling has been shown to contribute to social and economic development through increased productivity and through job creation (Arvizu et al., 2011).

The economic incentives for decentralized, off-grid energy access are very important. In widespread regions of the developing world Africa, the cost to construct and maintain power lines from centralized power generation facilities is high and the roads necessary for transporting liquid or gaseous fuels are insufficient. As a result, small-scale, decentralized, renewable energy sources are becoming increasingly competitive. By utilizing a feedstock that is locally available many of the costs of

expanding existing power grids, building and maintaining new roads and operating vehicles to transport fuel can be reduced. The most promising fuel source could be biomass from agricultural waste (Ahmed et al., 2012).

Biomass has the potential to address many of the concerns related to our energy future. Wood, the most commonly used biomass, has long been an important source of energy, used in stoves and ovens for centuries. It was replaced by coal as the primary energy source during the Industrial Revolution for wealthy nations. Today, concerns over the future of fossil fuels and over environmental degradation mean that biomass may once again be an important energy resource by utilizing more advanced technologies (Prins, 2005). Energy from biomass accounted for 10.2% (50.3 EJ) of the total global energy supply in 2008 (Edenhofer et al., 2011; Chum et al., 2011). Investment in biomass power globally was USD 10.6 billion in 2011 (Ahmed, 2001).

The renewal of interest in utilizing biomass worldwide as an energy fuel is due to a number of factors: First, technological advancements in the production and conversion of agricultural products have allowed yields to be higher and prices to be lower, making bio-derived electrical generation more competitive with fossil fuel-based energy generation. Second, concern over greenhouse gas emissions from conventional fuel sources has stimulated interest in carbon neutral energy resources and conversion technologies. Biomass-derived energy can be produced sustainably, unlike fossil fuel-derived energy. The carbon emitted during the conversion and combustion of biomass is offset by carbon taken up during the plant's growth (Muradov and Veziroglu, 2008). Encouraging biomass production for energy generation can lead to increased biodiversity,

as well as encouraging the cultivation of land not suitable for food production. Third, utilizing domestic and indigenous biomass sources allows for a more stable energy future and reduces import dependence (Chum et al., 2011). Finally, the number of countries with policies demanding increasing utilization of renewable energies to replace conventional fossil fuel-based energy has increased from 89 countries in 2009 to 118 countries in 2011 (Ahmed et al., 2001). These technological, economic, political, and environmental incentives for reducing dependence on conventional energy sources make biomass-derived fuels an attractive alternative, renewable, and sustainable energy source for use in more advanced conversion techniques.

By increasing the energy potential of biomass through one of many available conversion methods, biomass-derived energy can be used for more than just heating and cooking (Belgiorno et al., 2003). It can be used in any of the four end use markets of energy: power generation, transportation, heating and cooling, and rural/off-grid energy services (Ahmed, 2001). While biomass is readily available in most agricultural settings, it is rarely in a form that can be utilized efficiently with existing equipment in a facility. For example, woodchips from a farm might be usable in a hog-fuel boiler, but the equipment needed to convert the boiler to use this energy source would be cost prohibitive. In order to properly utilize the energy potential of the biomass in existing equipment and applications, it must be converted into a more readily usable fuel (Rajvanshi, 1986). Unfortunately, there are few economic incentives for the wide scale use of biomass gasification, as natural gas prices remain low.

There are four conversion methods for biomass into energy. These are direct combustion, thermochemical processing, biochemical processing and agrochemical processing (Chum et al., 2011). Direct combustion is the burning of biomass in the presence of oxygen to convert the chemical energy in the biomass to heat, mechanical power, or electricity. This energy can be used in stoves, furnaces, boilers, and steam turbines (Ni et al., 2006). In sub-Saharan Africa alone, 650 million people rely on direct combustion of biomass for heating and cooking yet this type of combustion generally has efficiencies ranging between 10-30% (Ahmed, 2001; Ni et al., 2006). Utilizing other conversion methods could lead to a more sustainable and efficient use of the biomass for a wider variety of applications. Thermochemical and biochemical conversion of biomass have the highest potential for hydrogen production from biomass. Biochemical conversions include bio-photolysis, microbic digestion, and fermentation and generally result in ethanol and methane production (Ni et al., 2006). Agrochemical application of biomass as an organic fertilizer is a common use of compost.

There are four major thermochemical conversion processes: gasification, pyrolysis, supercritical fluid extraction, and direct liquidification (Demirbaş, 2002). The conversion method studied in this work is a thermochemical conversion process. Gasification and pyrolysis can both produce gaseous fuels through the high temperature processes but pyrolysis can also be used to produce liquid oils or solid charcoal. Unlike pyrolysis which takes place without oxygen, gasification is carried out in the presence of some oxygen (Ni et al., 2006). Gasification is the partial oxidation due to heating of biomass to form a gas mixture rich in hydrogen ($H_2$) and carbon monoxide (CO) with

small amounts of methane ($CH_4$) and other light and heavy hydrocarbons (Belgiorno et al., 2003). A wide range of biomass can be gasified provided the ash content and the moisture content are both reasonably low. Wood, charcoal, and coal have the best combination of properties for successful gasification but other agricultural waste such as corn cobs, coconut husks, and switchgrass have been used in gasification systems (Ni et al., 2006; Demirbaş, 2002). By using biomass locally available to a community, the costs of small-scale distributed energy through biomass gasification are significantly lower than energy from utility-scale energy production facilities (greater than 1 MW). As biomass is uniformly distributed and can be processed into fuel locally, it is an attractive solution for distributed and decentralized energy generation in remote villages and communities (Buragohain et al., 2010). By producing useful electricity and heat close to the consumer, transportation costs and transmission losses are also reduced (Ahmed et al., 2012). However, variability in feedstock, moisture content, tar generation, and particulate matter emissions hinder the implementation of gasification (Akudo, 2008).

Unfortunately, biomass gasification is not a completely clean energy source. The conversion of biomass to energy via gasification and utilization in an engine, boiler or turbine produces semi-volatile hydrocarbon compounds, typical gaseous combustion products, and solid and gaseous contaminants. Particulate matter (PM) is generated and emitted during the conversion and combustion of biomass from integrated gasifiers (Belgiorno et al., 2003). Hydrocarbon emissions, particularly volatile organic compounds and polyaromatic hydrocarbons, are dangerous to respiratory health, causing diseases such as asthma (Nielsen et al., 1996). Compounds such as benzene, toluene, m- and o-

xylenes, ethylbenzene and naphthalene generated during gasification cause cancer, liver problems and neurological damage while particulate matter has detrimental effects on human's respiratory health and adds to environmental pollution (Nielson et al., 1996). Directive 2008/50/EC set forth from the European Parliament addresses many environmental pollutants that are generated through gasification, including nitrogen dioxide ($NO_2$), $PM_{10}$, $PM_{2.5}$, volatile organic compounds (VOCs). The European Unions' directive 2004/107/EC mandates target values for, among other elements, polycyclic aromatic hydrocarbons, some of which may be emitted from gasification systems. While these European directives and federal regulations from the US government give target ambient air limits in surrounding areas, systems used in developing countries for rural electrification may not be monitored or regulated as stringently. The efficiency of the system to reduce these contaminants before they are emitted into the environment is very important. Furthermore, some byproducts of biomass gasification, such as tars, indicate wasted energy in the conversion of the biomass to energy and they can be harmful to downstream components even if they are consumed during combustion.

Efficient removal of tars is the major barrier to wide scale commercialization of biomass gasification systems (Maniatis, 2008). Tar is generally accepted to be defined as aromatic organics produced during thermal or partial oxidation of biomass that condense under operating conditions in the system with molecular weight greater than benzene (Milne et al., 1998). Tar compounds in the vapor stage condense during gas cooling on downstream components of the system such as transfer lines, boilers, or engine inlets (Milne et al., 1998). In order to improve technology to make gasification a more

competitive energy source both economically and environmentally, the energy balance of the entire gasification and electrical generation system must be better understood. Understanding the composition and concentrations of contaminants in the producer gas can help manufacturers improve designs and optimize entire systems while protecting human health and minimizing environmental damage. Whereas many studies have looked at contaminants from biomass gasification, little has been done to see how they evolve as syngas or producer gas is consumed in an engine.

### 1.2. Research Objectives

This research quantifies and characterizes the products generated at various sampling points in a small-scale biomass gasifier and electrical generation system under different generator loading conditions. Producer gas is generated using The Power Pallet, a small-scale biomass gasifier commercially available from All Power Labs, Inc. The gasifier system uses a modified Imbert downdraft reactor with a cyclone and packed bed filter followed by a Kubota spark-ignited engine with natural gas head to generate electricity with the 10 kW Mecc Alte generator.

The primary objectives of the study are: (1) to quantify key contaminants present in producer gas from the small-scale downdraft gasifier operating on woodchips, (2) to determine to what extent these contaminants are eliminated by the engine, and (3) to evaluate the energy balance of the small-scale gasifier-generator system.

Key contaminants considered in the research include aromatic hydrocarbons, the foundation of tar generated by biomass gasification and particulate matter which includes

solid components like soot, ash, and fragmented materials as well as heavier tar species. The ratio of organic carbon to elemental carbon in the particulate matter is measured to better understand the composition of the particulate matter emissions. Gas composition, temperature, pressure, and flow measurements aid in the understanding of the gasifier's thermal efficiency and are essential for thermodynamic analysis of the system. By sampling from three strategic locations in the gasifier system, this study determined the filter's and the engine's ability to remove harmful compounds while monitoring the overall system efficiency and operating conditions.

# 2. Literature Review

## 2.1. Introduction to Gasification

Gasification has a long history having been first discovered in both England and France, independently in 1798 (Reed and Das, 1988). A wide variety of organic material can be gasified such as wood, agricultural residues, peat, coal, anthracite, oil residues and municipal solid waste (Prins et al., 2007). Beginning in the 1800s, gasification was used to produce fuel from coal and peat to be used in street lamps, internal combustion engines and other forms of transportation in Europe and the US. The first commercially available gasifier was produced in France in 1840 and with the addition of an engine in 1878 could be used for electrical generation and transportation (Wei, 2005). Gasification saw renewed interest as a means of generating electricity beginning in the 1900s.

When petroleum supplies for civilians were scarce during both world wars but particularly during World War II, gasification became much more common (Turare, 2002). As petroleum prices increased and supplies diminished, over a million vehicles were converted to utilize fuels generated through gasification worldwide (Reed and Das, 1988). Once petroleum supply levels and prices returned to normal, interest in coal gasification again waned. Furthermore, the discovery of large reserves of natural gas and the construction of pipelines to transport it displaced manufactured gas for heating and lighting.

Gasification has been plagued by high costs, high user demands, and low efficiency preventing it from becoming a widely used energy resource. Interest has once again increased in gasification technologies, with less focus on coal gasification and more

on biomass gasification. Biomass has gained attention as a renewable energy source due to concerns over the future of fossil fuel supplies and environmental sustainability. With the introduction of the Kyoto protocol in 1997, gasification of biomass gained more interest as a method of reducing net carbon dioxide emissions (Prins et al., 2007). Biomass gasification has been estimated to potentially supply between one-quarter and one-half of the world's energy demands by the middle of the 21$^{st}$ century (Ruth et al., 2013). It is important to understand if biomass can be gasified as efficiently as coal with respect to energy savings and environmental degradation.

Gasification is the process of partially oxidizing carbonaceous material into gaseous mixtures of hydrogen, carbon monoxide and other hydrocarbons through the application of high temperatures (>700°C) and with controlled additions of either air, oxygen or steam. By controlling the gasifying agent, the carbonaceous material is burned sub-stoichiometrically to prevent combustion and producer gas or syngas is created. Syngas typically describes gas that is created without nitrogen through pure oxygen or steam gasification, while producer gas generally has nitrogen from gasification with air. Gasification is carried out with equivalence ratios or the fraction of stoichiometric air, of approximately 0.25. Gasification can be used to convert coal, petroleum, biomass or biofuels into producer gas or syngas, which can then be used in a variety of applications. For some materials, gasification is preferred over direct combustion as the gas can be combusted at higher temperatures and because it can be used in internal combustion engines, turbines and fuel cells. Furthermore, gasification can refine out many of the corrosive ash elements present in the feedstock like chloride and potassium.

### 2.2. Gasification process

Gasification depends on both high temperatures and the oxidizing agent reacting with the carbonaceous material to be gasified. Air, oxygen or steam can be used as the oxidizing agent and can react with the material to be gasified in a number of different ways. Flow between the gasifying agent and the material to be gasified can be co-current flow, countercurrent flow, crosscurrent, or entrained flow. There are two major types of gasification reactors using different aerodynamics: fixed bed which maintains a steady bed of biomass and fluidized bed where the biomass is moved around with a material like sand within the reactor. Figure 1 shows the breakdown of various types of reactor designs and their respective market shares in 2005.

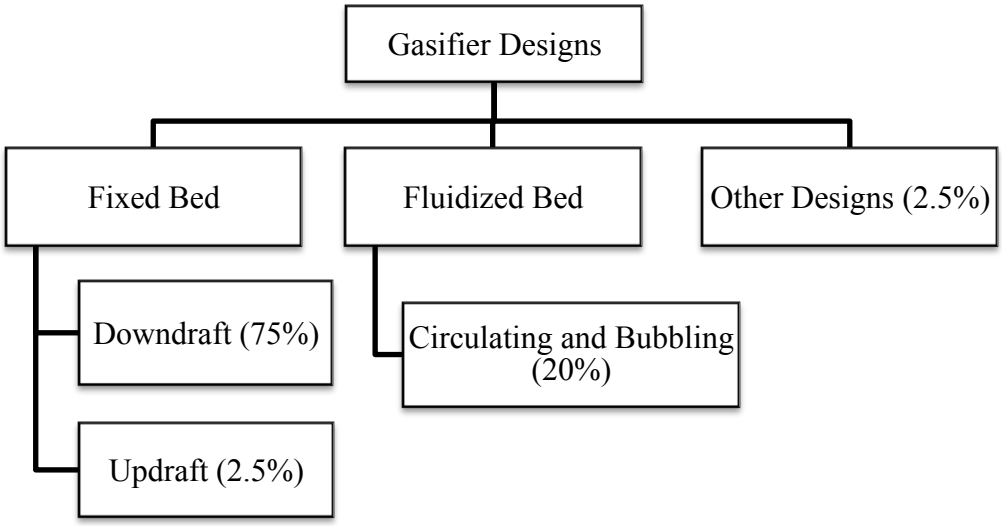


*Figure 1: Types of Gasification reactors, percentages indicate market share in 2005 (Wei, 2005)*

Fixed bed reactors can be either downdraft, which has co-current flow where the

biomass and oxidizing agent flow in the same direction, or updraft, which has countercurrent flow such that the biomass and oxidizing agent travel in opposite directions. In a downdraft gasifier, the feedstock is introduced through the top of the reactor and the gasifying agent enters through a grate in the side of the reactor. Downdraft gasifiers offer low sensitivity to charcoal and tar in the fuel and are able to quickly adapt to various gas production loads but they cannot tolerate very small particle fuels. There are two major varieties of vertical downdraft gasifiers: a stratified reactor, which has uniform width throughout the reactor or an Imbert reactor, which has a throated restriction in the combustion zone (Belgiono et al., 2003).

Updraft gasifiers are designed such that the feedstock and the gasifying agent travel in opposite directions, i.e. counter-current flow. The biomass derived gaseous fuel generally leaves from the top of the reactor as the solid feedstock travels downwards. The major advantages of updraft rectors are the small pressure drop, good thermal efficiency, and low tendency toward slag formation. Unfortunately, updraft gasifiers have greater sensitivity to tar and moisture in the feedstock, they cannot adapt gas production as quickly, and they require a long start up before they can run downstream components like IC engines (Rajvanshi, 1986). Overall the concentration of contaminants is significantly higher in updraft gasifiers than downdraft gasifiers and as a result they are uncommonly used.

The most notable advantage of downdraft gasification is the reduction in tar concentration. Downdraft gasifiers produce significantly lower tar concentrations than updraft gasifiers due in part to the increased residence time in the high temperature

combustion zone. The high temperature region in the reactor is useful for thermally cracking much of the tars into incondensable gaseous tars and water that is easily dropped out of the biomass derived gaseous fuel (Prins, 2005; Maniatis, 2008; Sheth and Babu, 2009). Producer gas from updraft gasifier leaves the reactor at fairly low temperatures (70-300°C) leading to more tar condensation in the gas stream than other higher temperature reactors. Furthermore, due to the aerodynamic movement in an updraft gasifier, tars coming off the feedstock during pyrolysis become entrained in the gas flow as the gas moves upwards through the cooler zones of the reactor. Again, the result is very high tar concentrations in the gas produced (Belgiorno et al., 2003). These high concentrations of tar limit the usability of the fuel in downstream applications like engines and turbines (Ståhlberg et al., 1998). Additionally, particulate matter concentrations are much higher in updraft reactors due to the aerodynamics of the gases. Due to the high concentration of contaminants, very few updraft gasifiers are being produced commercially, accounting for about 2.5% of the gasifier market in Europe, the US, and Canada while downdraft designs account for 75% (Maniatis, 2008).

In gasification reactors, the feedstock goes through four distinct conversion zones: drying, pyrolysis, reduction, and combustion. The highest temperature is reached in the combustion zone and can be as high as 1200°C (Belgiorno et al., 2003). The four distinct regions of the gasification process can be seen in Figure 2 for both downdraft and updraft fixed-bed reactors. The four processes that result in gasification happen in distinct regions of fixed-bed reactors. In other reactors designs, such as fluidized beds, the four processes are more difficult to distinguish due to the aerodynamics but the same

processes occur nonetheless (Rajvanshi, 1986).

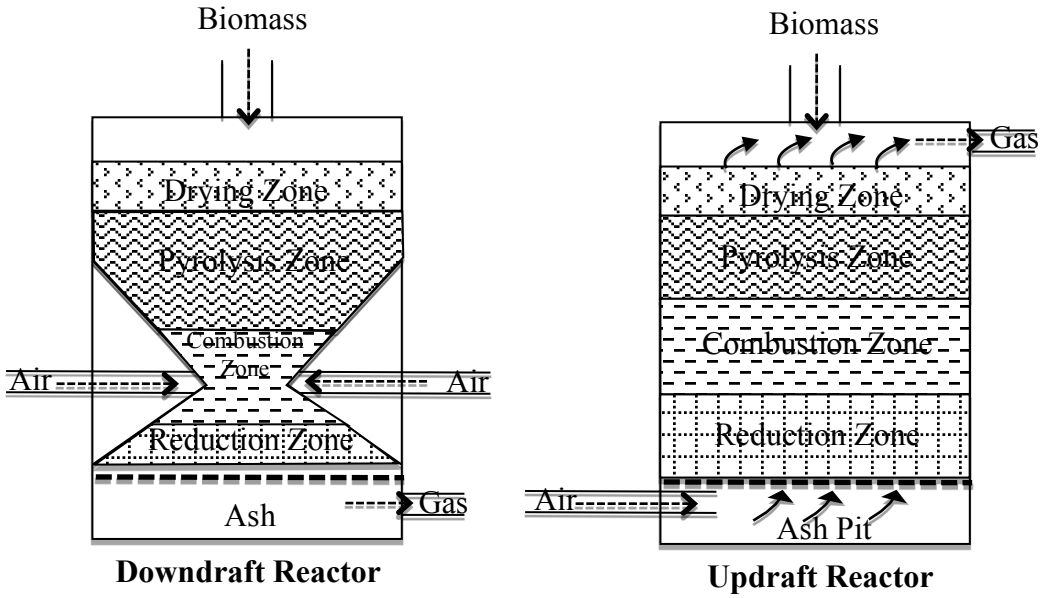


*Figure 2: Fixed-Bed Reactors (Akudo, 2008)*

Drying involves driving off moisture from the feedstock. By heating the material above 100°C, the entrained moisture is converted to steam. In subsequent conversion processes in the reactor, some of this steam is converted to hydrogen while some remains as water vapor in the resulting gaseous fuel. This moisture is easily dropped out of the gas flow before downstream applications (Rajvanshi, 1986). During drying, feedstocks do not undergo any decomposition (Turare, 2002).

In the pyrolysis zone, the feedstock undergoes thermal decomposition without oxygen at about 200°C. The feedstock is decomposed into volatile gases and char (Akudo, 2008). The gaseous products of pyrolysis are primarily $H_2$, $CO_2$, CO, $CH_4$, $C_2H_6$, $C_2H_4$ with trace amounts of larger gaseous organics and water vapor. The ratios of the

products from this process depend on the feedstock supplied to the reactor (Yang et al., 2007). Since pyrolysis is an endothermic process, the heat is provided from subsequent stages of the gasification process (He et al., 2006). The main thermal degradation process for biomass during pyrolysis can be represented as follows (Akudo, 2008):

$$C_6H_{10}O_5 + \text{Heat} \rightarrow {}_yC_xH_z + {}_qC_xH_nO_k + CO + C$$

In all reactor designs, there is always a low temperature pyrolysis zone, which generates tar, and the gas produced from this region has low heating value (3.5-8.9MJ/$m^3$) (Demirbaş, 2002).

After the feedstock is pyrolyzed, it enters the oxidation or combustion zone. In this region of the reactor, the gasifying agent enters the starved oxygen environment and oxidation occurs between 700-1200°C. The oxidation reactions are as follows (Demirbaş, 2002; Akudo, 2008):

$$C+O_2 \rightarrow CO_2 \ (+406 \text{ MJ/kmol})$$

In this heterogeneous reaction, the carbonaceous material in the feedstock reacts with the oxygen in the gasifying agent to produce carbon dioxide and heat (Turare, 2002). Another important reaction which takes place in this region is as follows:

$$2H_2+O_2 \rightarrow 2H_2O \ (+242 \text{ MJ/kmol})$$

Here, the fuel's hydrogen reacts with the oxygen in the gasifying agent to produce water vapor and heat.

After oxidation, the feedstock enters the reduction zone. If the feedstock in the reactor is biomass, the lignocellulosic compounds undergo thermochemical decomposition to form char and volatiles in the oxygen-starved environment. The

following reactions take place in this region of the reduction zone of the reactor (Demirbaş, 2002):

Boudouard reaction:

$$C + CO_2 \rightarrow 2CO \ (-172.6 \text{ MJ/kmol})$$

Water-gas shift:

$$C + H_2O \rightarrow CO + H_2 \ (-131.4 \text{ MJ/kmol})$$

Water shift reaction:

$$CO + H_2O \rightarrow CO + H_2 \ (+41.2 \text{ MJ/kmol})$$

Methane production reaction:

$$C + 2H_2 \rightarrow CH_4 (+75 \text{ MJ/kmol})$$

Due to the nature of these reactions, the products from the reduction zone are at a lower temperature than the reactants (Wei, 2005). For complete gasification, all the carbon must be burned or reduced to carbon monoxide and the only solid remaining is ash and char. Ash is a noncombustible mineral material and char is unburned carbon (Turare, 2002). The main gaseous products of these reactions are $H_2$, $CO_2$, CO and $N_2$ if the biomass is gasified with air.

The other major category of reactor is fluidized bed reactors. These reactors use a bed of fine solids such as silica sand as a heat carrier. The gasifying agent transforms the bed of sand into a fluid-like substance by flowing upward through it. The feedstock to be gasified enters the reactor where it interacts with the hot fluidized bed and the oxidizing agent such that the gaseous fuel exits through the top of the reactor and ash is removed from the bottom (Belgiorno et al., 2003). The two variations of fluidized bed reactors are

circulating bed reactors and bubbling bed reactors. In a circulating fluidized bed reactor, the gasifying agent moves at 5-10 m/s so that the expanded bed of the sand occupies the entire reactor and the gas phase reaction occurs within the fluidized bed. Circulating fluidized beds can be operated at higher pressures and can therefore be used easily with gas turbines (Sethuraman, 2010). In a bubbling bed reactor, the gasifying agent only moves at 1-3 m/s and the fine silica sand expands to fill only a portion of the reactor. Fluidized bed reactors can be used with catalytically active bed materials such as dolomite to improve the ash and tar removal in the resulting gas. The major advantage of fluidized beds over fixed-bed reactors is the improved removal of ash and tar. Tar concentrations are lower in fluidized bed reactors than updraft reactors due to the high temperature thermal cracking that takes place in the fluidized bed. Furthermore, by creating a high centrifugal field within the reactor, ash is also reduced (Akudo, 2008). Unfortunately, fluidized bed reactors are slower to start up, have low carbon conversion (~90%), and the high temperature of the reactions can lead to issues with alkali metals slagging downstream operations. Table 1 shows some of the differences in operating parameters for downdraft fixed-bed reactors and fluidized-bed reactors.

*Table 1: Typical Characteristics of Fixed-Bed and Fluidized-Bed Gasifiers (Quaak et al., 1999)*

| **Characteristic** | **Fixed-bed downdraft** | **Fluidized-bed** |
|---|---|---|
| Fuel: size (mm) | 10-100 | 0-20 |
| ash content (% wt) | <6 | <25 |
| Operating temperature (°C) | 800-1,400 | 750-950 |
| Control | simple | average |
| Turndown ratio | 4 | 3 |
| Construction material | mild + refractory | Heat-resistant steel |
| Capacity ($MW_{th}$) | <2.5 | 1-50 |
| Startup time | minutes | hours |
| Attendance | low | average |
| Tar content ($g/Nm^3$) | <3 | <5 |
| LHV ($MJ/Nm^3$) | 4.5 | 5.1 |

### 2.3. Biomass Gasification

Gasification can be applied to a variety of feedstocks including coal, biomass, black-liquor, municipal solid waste, and refuse derived fuel. Biomass gasification, however, has the potential to renewably meet a significant portion of the world's energy needs without net emissions of greenhouse gases. Biomass encompasses a wide range of materials including woodchips, wheat straw, sawdust, cornhusks, coconut husks, barley straw, rice hulls, switchgrass, and wood pulp (Ni et al., 2006). Since most biomass feed-stocks that are suitable for gasification are agricultural waste, there is less concern over food products being diverted to energy generation than there is with such technologies as ethanol production.

Biomass gasification generally takes place with air as the gasifying agent, although steam and pure oxygen are also possible gasifying agents. Producer gas generated with air is about 50% nitrogen and has a lower heating value (LHV) between 2.5 to 8.0 $MJ/Nm^3$. Gasifying in pure oxygen or steam would result in syngas virtually

free of nitrogen with a LHV of 10 to 20 MJ/$m^3$. Despite the higher energy density of gas generated without nitrogen, gasification with air is significantly cheaper and simpler; therefore gasification with air is much more common, particularly for decentralized energy generation (Wei, 2005).

### 2.4. Effects of Feedstock Properties on Gas Products

In order to understand how the products of the gasification process change, some properties of the biomass feedstock must first be discussed. Although there are a wide variety of biomass feedstocks available, including wood, crops and animal waste, the characteristics of the biomass such as its moisture content, ash content, elemental composition, energy density, and volatile matter determine its performance as a fuel.

The first property to be discussed is moisture. There are two types of moisture in biomass. The first is intrinsic moisture, which is the moisture of the material without any weather effects. The second is extrinsic which is the moisture associated with weather during the harvesting and storage of the biomass. Moisture content is expressed as a percentage of the mass that is water, either on a dry basis, a wet basis or a dry and ash-free basis. Feedstocks can have a wide range of moisture content depending on both the type of biomass and the conditions in which it was grown and harvested. For example, cereal grain has a moisture content of less than 10% on a wet basis while forest residue can have moisture content in the range of 50 to 70% on a wet basis but these values can vary depending on weather conditions (Quaak et al., 1999). In order for the gasification process to be self-sustaining in a reactor, biomass must be reasonably dry. Excess

moisture also affects the heating value of the producer gas (Akudo, 2008). Biomass gasified in a downdraft fixed bed reactor generally needs to be below 30% moisture content on a dry basis in order to produce high quality gas.

Another important property of biomass is ash content. Ash is the inorganic, non-combustible material in a fuel. Ash includes minerals taken up by the plant during growth such as potassium, calcium, and phosphorus. Ash released from the biomass during gasification can sometimes be used as a fertilizer. Large ash particles fall into the ash pit in the reactor and this type of ash is referred to as bottom ash. Small ash particles become entrained in the gas flow and are referred to as fly ash. Fly ash must be removed from the syngas or producer gas prior to downstream applications as it is generally composed of high concentrations of heavy metals which can damage components (Pitman, 2006). Ash content is quantified in the same manner as moisture content, as a percentage on a wet, dry or dry and ash-free basis but is most commonly expressed on a dry basis. High temperature gasification, common in fluidized bed reactors, can cause heavy alkali metals in the ash to melt damaging the reactor and downstream components if proper cleanup technologies are not used (Quaak et al., 1999). Ash accounts for about 1 to 20% of the biomass' mass on a dry basis.

Elemental composition is another important property of biomass. The three main constituents in plant biomass are lignin, which accounts for 15-25% of the biomass, hemicellulose, which is 23-32% of the biomass, and cellulose, which is the remaining 38-50% of the biomass. Lignin is a complex aromatic structure with very high energy content. Hemicellulose is a polymer with 5 and 6 carbon sugars. Cellulose is a polymer of

glucose, which is a very good biochemical feedstock. The elemental composition of lignocellulosic biomass is fairly uniform on an ash-free basis consisting primarily of carbon, oxygen and hydrogen (Quaak et al., 1999). There is very little nitrogen and sulfur in woody biomass. The atomic O/C ratio of biomass is between 0.4 to 0.9 while coal has O/C ratios between 0 and 0.3 (Prins et al., 2007). The average range of each element's weight percent on a dry and ash-free basis is shown in Table 2.

*Table 2: Elemental Composition of Typical Biomass (BTG, 1987; Quaak et al., 1999)*

| **Element** | **Symbol** | **Weight percent (dry and ash-free basis)** |
|---|---|---|
| Carbon | C | 44-51 |
| Hydrogen | H | 5.5-6.7 |
| Oxygen | O | 41-50 |
| Nitrogen | N | 0.12-0.060 |
| Sulfur | S | 0.0-0.2 |

The heating value of biomass is the value of the energy chemically bound in the fuel and is given in terms of energy per unit mass (J/kg). For wood from short rotation coppice like willow, poplar and forest residue, the heating value is approximately 18 MJ/kg on a dry and ash-free basis but can vary from 17-21 MJ/kg on a dry and ash-free basis for most biomass feedstocks (McKendry, 2002). Heating value can be measured with either water in the products in the vapor state or in the liquid state and these two common heating values are referred to as the lower heating value (LHV) and higher heating value (HHV), respectively. As mentioned, biomass has intrinsic moisture, which is inherent to the feedstock. This moisture is released during the drying process in the reactor and the evaporated water absorbs some of the heat released during gasification. As a result, the net lower heating value of the fuel decreases with increasing moisture

content. Figure 3 shows the general relationship between caloric value (LHV and HHV) and the moisture content for the biomass (Quaak et al., 1999).

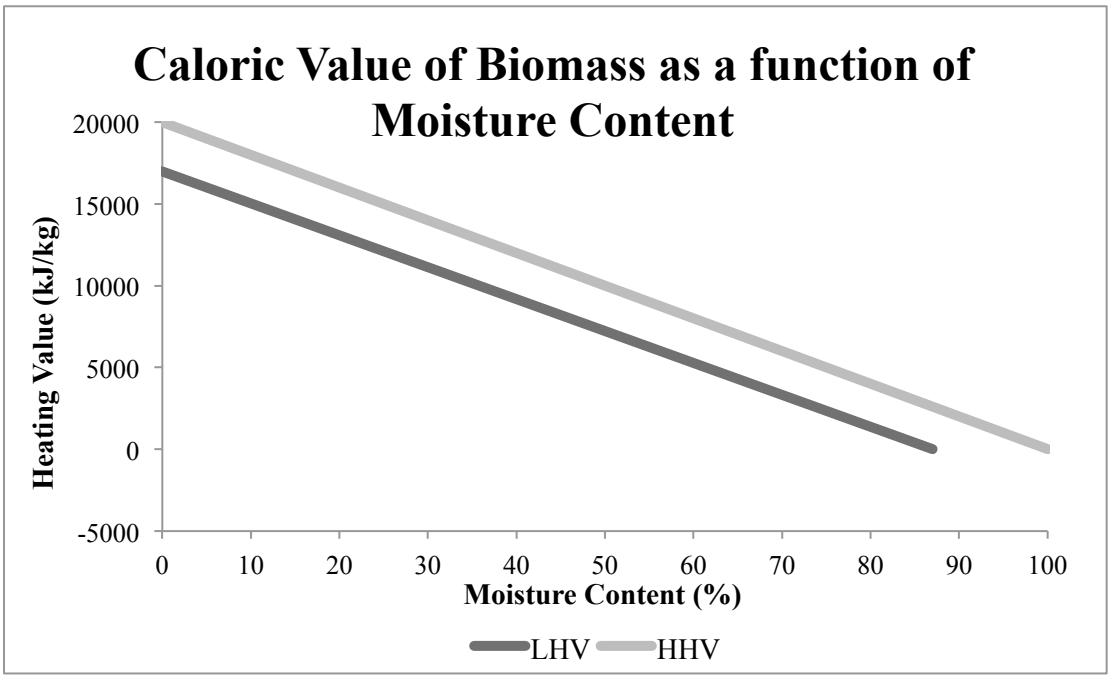


*Figure 3: Caloric Value versus Moisture Content (Quaak et al., 1999)*

Bulk density is another important characteristic of biomass as it indicates which type of reactor is applicable for gasification. Bulk density describes the weight of biomass per unit volume and is generally expressed on an oven-dry basis as if the moisture content were zero. Biomass can have a wide range of bulk densities from 150 to 200 kg/m$^3$ for cereal grain straws to 600 to 900 kg/m$^3$ for solid wood. Combining the bulk density and the heating value gives the energy density, which is the energy per unit volume. (Quaak et al., 1999).

Volatile matter concentrations are also important in regards to biomass. When biomass is heated to 400 to 500°C, the volatile matter is released and char is formed.

Biomass is about 80% volatile matter while coal has volatile matter content ranging from 5% for lignite coal up to 27% for anthracite coal (Prins et al., 2007; Quaak et al., 1999).

All of these characteristics such as moisture content, ash content, heating value, energy density and volatile matter are important to consider when determining which biomass would be an appropriate feedstock for energy generation in a particular reactor design. Table 3 shows lower heating values and moisture content on a wet basis and ash content on a dry basis for some commercially used biomass feedstocks.

*Table 3: Properties of Various Biomass Feed stocks (Quaak et al., 1999)*

| **Type** | **Lower Heating Value $LHV_w$ (kJ/kg)** | **Moisture Content $MC_w$ (%)** | **Ash Content $AC_d$ (%)** |
|---|---|---|---|
| Bagasse | 7,700-8,000 | 40-60 | 1.7-3.8 |
| Cocoa husks | 13,000-16,000 | 7-9 | 7-14 |
| Coconut shells | 18,000 | 8 | 4 |
| Coffee husks | 16,000 | 10 | 0.6 |
| *Cotton Residues* | | | |
| Stalks | 16,000 | 10-20 | 0.1 |
| Gin trash | 14,000 | 9 | 12 |
| *Maize* | | | |
| Cobs | 13,000-15,000 | 10-20 | 2 |
| Stalks | | | 3-7 |
| *Palm-oil residues* | | | |
| Fruit stems | 5,000 | 63 | 5 |
| Fibers | 11,000 | 40 | |
| Shells | 15,000 | 15 | |
| Debris | 15,000 | 15 | |
| Peat | 9,000-15,000 | 13-15 | 1-20 |
| Rice husks | 14,000 | 9 | 19 |
| Straw | 12,000 | 10 | 4.4 |
| Wood | 8,400-17,000 | 10-60 | 0.25-1.7 |
| Charcoal | 25,000-32,000 | 1-10 | 0.5-6 |

Characteristics of the feedstock determine which reactor is most applicable for gasification. For example, updraft reactors can tolerate higher moisture and ash contents

than downdraft reactors. The reactor type also dictates many of the characteristics of the resulting producer gas or syngas and therefore the applicable end-use technologies. For example, updraft reactors produce more tar than downdraft reactors and would require more gas cleanup before the syngas or producer gas were to be used in an engine or turbine. Table 4 shows tolerances for many properties of wood biomass in both downdraft and updraft fixed-bed reactors and some of the properties of the resulting gases.

*Table 4: Characteristics of Various Gasifiers (Quaak et al., 1999)*

| **Characteristics** | **Downdraft Fixed Bed** | **Updraft Fixed Bed** |
|---|---|---|
| Fuel (wood) | | |
| Moisture Content $MC_w$ (%) | 12 (max 25) | 43 (max 60) |
| Ash Content $AC_d$ (%) | 0.5 (max 6) | 1.4 (max 25) |
| Size (mm) | 20-100 | 5-100 |
| Gas exit temperature (°C) | 700 | 200-400 |
| Tar ($mg/Nm^3$) | 15-500 | 30,000-150,000 |
| Sensitivity to load fluctuations | Sensitive | Not sensitive |
| Turndown ratio | 3-4 | 5-10 |
| $h_{HG}$ full load (%)[a] | 85-90 | 90-95 |
| $h_{CG}$ full load (%)[b] | 65-75 | 40-60 |
| Producer gas LHV ($kJ/Nm^3$) | 4.5-5.0 | 5.0-6.0 |

a. $h_{HG}$ Hot gas efficiency. This takes into account the heat contained in the gas for heat applications.

b. $h_{CG}$ Cold gas efficiency. The gas will be cooled after leaving the gasifier to ambient temperature for engine and power applications.

Although the quality of the producer gas or syngas depends on the biomass gasified, the reactor design used, and the operating conditions during gasification the major constituents of producer gas are $N_2$, CO, $CO_2$, $H_2$ and $CH_4$ with small concentrations of higher hydrocarbons, tars, and particulate matter. Syngas has the same

major constituents except for $N_2$. In a downdraft gasifier, gasifying woodchips, the approximate gaseous concentrations of the major constituents of the resulting gas are shown in Table 5.

*Table 5: Producer Gas Composition from Downdraft Reactors (Hasler and Nussbaumer, 1999)*

| **Producer Gas Constituent** | **Volumetric Concentration on a Dry Basis (%)** |
|---|---|
| Nitrogen ($N_2$) | 35-60 |
| Carbon Dioxide ($CO_2$) | 11-13 |
| Hydrogen ($H_2$) | 15-21 |
| Carbon Monoxide (CO) | 10-22 |
| Methane ($CH_4$) | 1-5 |
| Higher Hydrocarbons ($C_xH_y$) | 0.5-2 |

For producer gas from a fixed bed downdraft reactor, Hasler and Nussbaumer (1999) report lower heating values in the range of 4.0-5.6MJ/$Nm^3$.

### 2.5. Tar Concentrations

One of the major stumbling blocks to commercial utilization of gasification for sustainable energy generation is the high concentration of tars in the resulting gaseous fuels. Tars are generally accepted to be all organic compounds with molecular masses greater than benzene. The organic compounds, generally assumed to be aromatics, characterized by high boiling points are produced in the higher temperature zones of the reactor (Milne et al., 1998). The major tar components are toluene, naphthalene, and phenol. Tars are very difficult to remove due to their properties. Failing to properly cleanup the gaseous fuel can lead to condensation, formation of tar aerosols, and polymerization that cause problems in downstream components (Kishore, 2009). Tar

concentrations in the biomass derived gas decrease with increasing temperatures in the reactor. There are also different types of tars which must be considered for cleanup methods. Primary tars, which are formed by decomposition of the building blocks of biomass, can change into secondary and tertiary tars through oxidation Reactors that gasify at low temperatures, such as updraft fixed bed reactors, have the highest concentrations of tar, mostly made up of primary tars (Rubou et al., 2009). Higher temperature reactors such as fluidized bed reactors have significantly lower concentrations of tars but the tars present are predominately secondary and tertiary tars (Milne et al., 1998).

Tar cleanup is vital for proper operation of downstream applications of the biomass-derived gas. Without proper gas cleaning, tars present in the gas stream can cool and condense on supply lines and within vital components of downstream mechanisms. Once cooled, the solid tars can cause clogs in valves and supply lines, can erode parts in engines and turbines, and can reduce the overall efficiency of the gasification system. Tars also clog filters, increasing the associated pressure drop across the filter and again reducing the efficiency of the system (Rabou et al., 2009).

Tars can be classified into five groups: GC undetectable tars, heterocyclic components, aromatic components, light polyaromatic hydrocarbons, and heavy polyaromatic hydrocarbons. GC undetectable tars, light polyaromatic hydrocarbons and heavy polyaromatic hydrocarbons are of most concern for condensation in downstream components. GC undetectable tars and heavy polyaromatic hydrocarbons condense at high temperatures, even at low concentrations, while light polyaromatic hydrocarbons

condense at intermediate temperatures. These heavy tars cause major fouling and increased maintenance when they condense out of the gas stream. Light tars, although less likely to condense, can pollute bleed water and aqueous scrubbers. One such light tar, naphthalene, is known to crystalize in engine inlets damaging parts and requiring service (Milne et al., 1998).

Tars have considerable heating value. In some reactor designs, tars concentrations account for only about 0.5% of the resulting gaseous fuel mixture yet account for 7% of the energy value. In coal gasification, a much more developed technology, tars are a useful fuel yet in biomass gasification they have only minor use due to the lower temperatures used (Milne et al., 1998). Unfortunately, most tar compounds have extremely high boiling points, making thermal destruction and utilization of the energy very difficult. Polycyclic aromatic hydrocarbons such as phenanthrene and anthracene are the most difficult to crack. These tars are always present in biomass and require long residence time in very high temperature environments, between 850°C to 1200°C, to crack thermally. There are a variety of different mechanisms for tar removal that can be employed in biomass gasification systems.

### 2.6. Particulate Matter

High concentrations of particulate matter in producer gas and syngas are also potential pit-falls of gasification for distributed energy applications. Soot, ash, and fragmented materials are a major contaminant in unfiltered producer gas and are a minor contaminant in engine emissions. Ash is a natural constituent of biomass but some ash

can become entrained in the gas flow after the volatile material is driven off. Bottom ash is the large ash particles that fall into the ash pit in the reactor. This ash is easily removed after many hours of operation and can be used as a fertilizer. Small ash particles become entrained in the gas flow and are referred to as fly ash. This type of ash must be removed from the syngas or producer gas as it is generally composed of high concentrations of heavy metals, which can damage downstream components and this type of ash cannot be used in fertilizers (Pitman, 2006). Very high temperature gasification such as in a fluidized bed reactor can cause heavy metals in the ash to melt damaging the reactor and possibly damaging downstream mechanisms (Quaak et al., 1999). There are a variety of different mechanisms for particulate matter removal that can be employed in biomass gasification systems.

### 2.7. Gas Cleanup Technologies

As there are significant contaminants in producer gas, it is essential to clean up the gaseous fuel before it can be used. The level of contamination of the producer gas or syngas is dependent on the reactor type, operating conditions, and feedstock. The approximate levels of contamination can be seen in Table 6 for downdraft and updraft fixed-bed gasifiers as well as for circulating fluidized bed reactors. While there are a wide range of contaminant concentrations, it is generally accepted that updraft fixed bed reactors produce about 100 g/Nm$^3$ of tars, fluidized bed reactors produce about 10 g/Nm$^3$ of tars, and downdraft fixed bed reactors produce about 1 g/Nm$^3$ of tars.

*Table 6: Gas Quality from Various Biomass Gasifier Reactor Designs (Hasler and Nussbaumer, 1999)*

| | **Fixed bed Downdraft** | **Fixed bed Updraft** | **Circulating Fluidized Bed** |
|---|---|---|---|
| Particles ($mg/Nm^3$) | 100-8,000 | 100-3,000 | 8,000-100,000 |
| Tars ($mg/Nm^3$) | 10-6,000 | 10,000-150,000 | 2,000-30,000 |

Failing to properly reduce solid and gaseous contaminants in the producer gas can lead to severe operational problems in downstream applications as well as reduced overall efficiency. There are two major categories of gas clean up technology for tar removal: physical cleaning and thermal/catalytic reforming. The five major mechanisms for particulate matter removal are inertial impaction, interception, diffusion, electrostatic deposition, and sedimentation (Hinds, 1999). Gas cleaning for the removal of particulate matter and tars can be categorized as wet scrubbing, dry or wet-dry scrubbing, or hot gas cleaning (Milne et al., 1998). Figure 4 shows a wide variety of gas cleaning technologies that are characterized in this way.

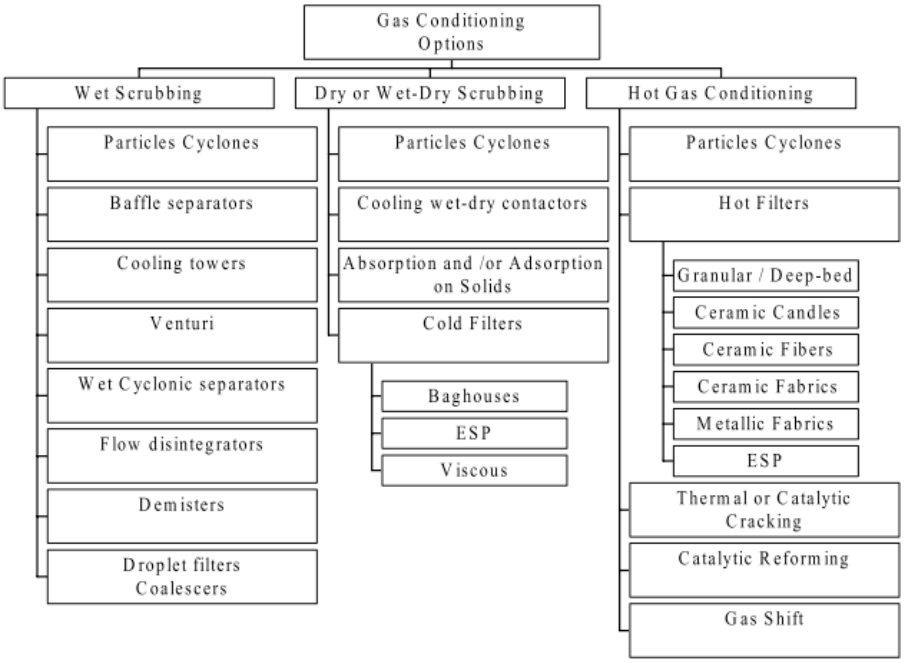


*Figure 4: Gas Conditioning Options (Milne et al., 1998)*

Some of the commonly used gas cleanup technologies in biomass gasification are shown in Table 7 with their operating temperature limits and their respective efficiencies for removing tars and/or particulate matter.

*Table 7: Gas Clean Up Method Efficiencies (Hasler and Nussbaumer, 1999)*

| | **Temperature (°C)** | **Particle Reduction (%)** | **Tar Reduction (%)** |
|---|---|---|---|
| Sand bed filter | 10-20 | 70-99 | 50-97 |
| Wash tower | 50-60 | 60-98 | 10-25 |
| Venturi scrubber | - | - | 50-90 |
| Rotational atomizer | <100 | 95-99 | - |
| Wet electrostatic precipitator | 40-50 | >99 | 0-60 |
| Fabric filter | 130 | 70-95 | 0-50 |
| Rotational particle separator | 130 | 85-90 | 30-70 |
| Fixed bed tar adsorber | 80 | - | 50 |
| Catalytic tar cracker | 900 | - | >95 |

Packed bed filters, also known as sand-bed filters, utilize neutral and non-reactive material such as sand or sawdust to cool the gas and condense tars from the gas stream. Particulate matter is also significantly reduced in a packed bed filter. The bed material must be selected to optimize removal of contaminants while maintaining a reasonable pressure drop. The material in the filter can be changed once it becomes saturated and either discarded or in some cases regenerated. Packed bed filters can be made with low cost filter material which is locally available making this a useful filtration method for gasification systems in rural and non-industrialized communities. Furthermore, many downstream applications of the fuel such as IC engines require the gas to be at ambient temperatures such that cooling the gas in this type of filter is an additional benefit (Pathak et al., 2007).

Cyclones or rotational particle separators remove solid particles and some tars from the gas stream. Gas enters the cyclone and due to changes in the internal geometry of the device, the gas is forced to rotate around the cylinder several times before exiting the top of the cyclone (Hinds, 1999). Large entrained particles, unable to adapt to the changing direction of the flow, leave the gas stream and collect in the bottom of the cyclone. Rotational particle separators have the advantage of being highly reliable, fairly low cost, and compact while maintaining a low pressure-drop across them. However, cyclones are not able to withstand high temperatures and they are not efficient at removing particles with diameters smaller than 2.5μm (Hasler and Nussbaumer, 1999). As most tar aerosol particles are smaller than 1 μm, cyclones are inefficient at removing tars from the gaseous fuel but very effective at removing fly ash (Kumar et al., 2009).

Fabric filtration is a common industrial method of reducing high dust concentrations. Large installations of fabric filters use fabric bags operating in parallel to achieve high efficiencies and process large volumes of gas. As the dust and some tars collect on the filter, collection efficiency increases but pressure-drop also increases. Overall, baghouses are very efficient and have a low pressure-drop but they cannot tolerate high temperatures and the bags must be replaced every 2-3 years (Hinds, 1999). Fabric filters can also remove tars by allowing tars to condense on the filter material, however the efficiency of tar removal is very low as the tar aerosols are small (Hasler and Nussbaumer, 1999).

Another cleanup method is scrubbers. Dry scrubbers clean the flue gas with sand while wet scrubbers use water or oil to clean the gas. In a wet scrubber, droplets of the fluid catch dust particles. The water or oil droplet with the now entrained particle is then removed via a drop tray. In a dry scrubber, tars condense on sand particles which can then be removed by the drop tray. The major advantages of scrubbers are that it they are adjustable for the emissions of the incoming gas and there is no fire risk as hot gas can be cooled in the scrubber. Unfortunately, scrubbers require considerable energy to operate properly, generate a great deal of waste water in the case of wet scrubbers, and are less than 95% efficient. Furthermore, wet scrubbers reduce the temperature of the product gas, decreasing the overall energy efficiency of the system, particularly if the downstream use of the gaseous fuel is a high temperature application (Kumar et al., 2009).

Electrostatic precipitators (ESP) are very efficient at removing particulate matter from producer gas and syngas. ESPs induce an electrical charge on particles in the gas

stream in order to efficiently attract them to the charged walls of the precipitator. ESPs have very high efficiency for removing particles and can be operated at high temperatures but they are ineffective at removing tars. Furthermore, ESPs require very high voltages to operate and their efficiency is dependent on the quantity of gas being cleaned (Hinds, 1999). As a result, ESPs are generally only used in very large-scale operations (Kumar et al., 2009).

Active in-bed catalytic materials are useful for converting tars in circulating fluidized bed reactors. Natural rock materials like olivine sand, limestone, and dolomite are useful in this application due to their porous calcined form. Dolomite, the most widely used catalytically active bed material, is especially active with up to 95% tar conversion and it is cheap and disposable. Tar reduction efficiency is determined by the porosity and surface structure of the catalyst, which is not homogeneous. Natural mineral catalysts can differ by region and their soft structure makes them subject to high attrition. Furthermore, natural mineral catalysts can be deactivated by carbon deposition and by re-carbonation when partial pressures if $CO_2$ are too high in the system. In-bed catalysts are able to significantly reduce tar concentrations but are not able to completely eliminate tar without secondary tar cleanup methods (Kumar et al., 2009).

Another method of tar removal is fixed bed tar adsorbers. These beds of catalytic material are generally carbonaceous materials like lignite or activated carbon and the gaseous fuel is filtered through the material after leaving the reactor. The small, irregularly shaped bed material has high surface area and can be used at various temperatures for optimal tar removal. Activated carbon is a cheap bed material and can

be produced locally in rural and non-industrialized communities. Once the bed material becomes laden with heavy tars it can be used as additional fuel in the reactor, reducing the solid waste from the system (Al-Dury and Sausan, 2009).

An emerging technology for tar and particulate matter cleanup is oil based gas washing (OLGA) developed by the Energy research Center of the Netherlands (ECN). The multiple-stage wet scrubber operates above the water dew point by using a special scrubbing oil to remove tar from the gaseous fuel and then feeds the tars back into the reactor. The oil is regenerated in a stripper column using hot air to separate tar from oil and the tars, entrained in the hot air stream, are fed back into the reactor with gasifying air to be fully destructed leaving essentially no waste. OLGA has demonstrated very high tar clean up efficiencies in both small-scale laboratory tests and large gasification systems. One major advantage of this system is the lack of contamination of waste water while thermally destroying tars in the reactor. Furthermore, OLGA has been shown to reduce concentrations of many of the harmful organic solvent compounds present in this type of gaseous fuel (Zwart et al.; Kumar et al., 2009).

The ranges of efficiencies for the gas clean up technologies described are shown in Figures 5 and 6 below. Unfortunately, the best cleanup technology for biomass derived gaseous fuels must be chosen based on the removal efficiency required, the availability of materials, the associated costs as well as the energy demands needed for successful operation so there is no solution which is best for all applications.

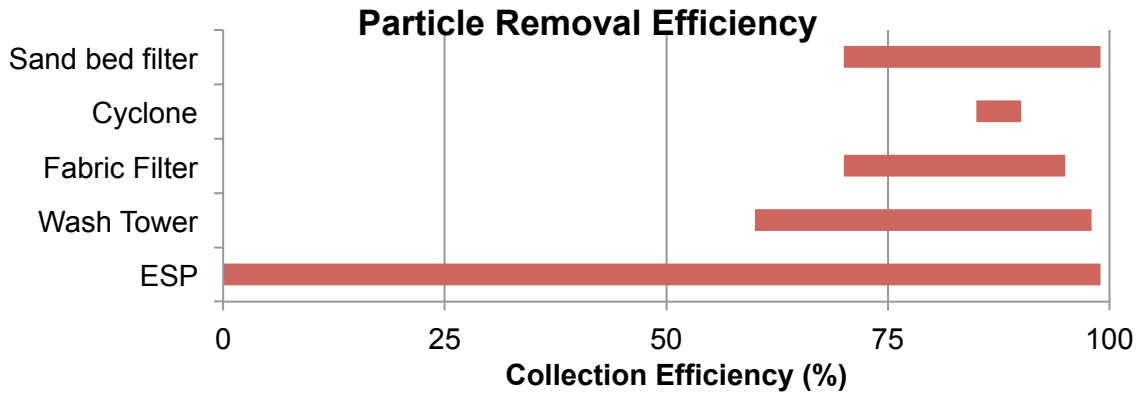


*Figure 5: Particle Removal Efficiencies (Hasler and Nussbaumer, 1999)*

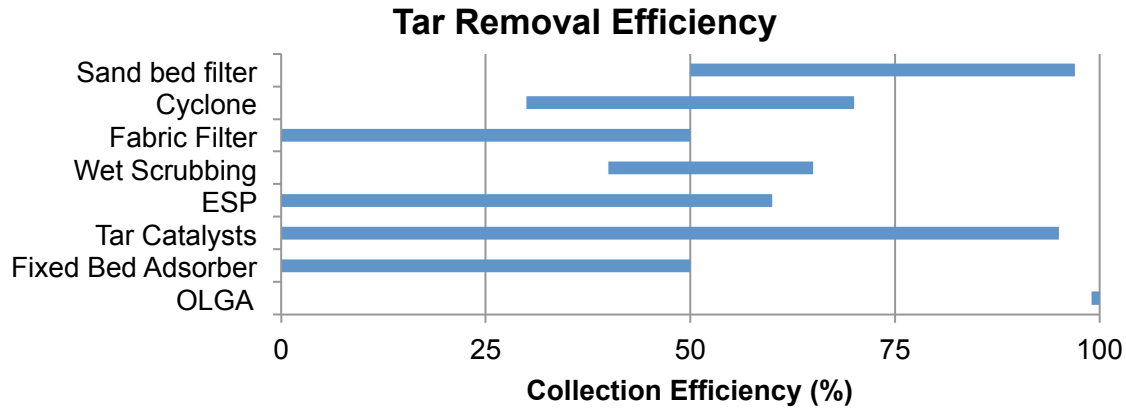


*Figure 6: Tar Removal Efficiency (Hasler and Nussbaumer, 1999)*

### 2.8. Hazardous Organic Solvents

Another contaminant in biomass derived gaseous fuels is organic solvents also referred to as volatile organic compounds (VOCs) and aromatic hydrocarbons. Organic solvents are carbon-based substances capable of displacing other substances. The National Institute of Safety and Health (NIOSH) classify many organic solvents as known carcinogens, neurotoxins and/or being harmful to reproductive health and the Occupation Safety and Health Administration (OSHA) regulate their emissions. The

hazardous organic solvents of most interest in biomass gasification systems are the BTEX compounds (benzene, toluene, ethylbenzene and xylenes). These compounds are useful fuels in coal gasification due to the high temperature cracking which takes place in the reactor but are of little use in biomass gasification and they are hazardous to human health and the environment (Milne et al., 1998).

Benzene is a natural constituent of crude oil, gasoline, and cigarette smoke. It is also found in manufacturing facilities of lubricants, dyes, detergents, and drugs. The major paths of exposure are inhalation, skin contact and indigestion primarily through contaminated drinking water. Benzene has been detected in the exhaust gas from many biomass gasification systems, occasionally at levels hazardous to workers in the facility and those in the immediate vicinity (Fuchs and Hofbauer). In internal combustion engines, engine capacity, and ignition timing affect benzene concentrations in the exhaust. One method of changing benzene concentrations in engine exhaust is through the use of oxidation catalysts (Department of Health and Human Services, 2007).

Toluene, another hazardous organic solvent present in producer gas and syngas, is a colorless liquid and a vapor in air at room temperature. It is often found in gasoline, paint, metal cleaners, adhesives, shellac, nail polish, and rust preventives however, it can be found in the emissions from a biomass gasification system at levels that are hazardous to human health (Department of Health and Human Services, 2007).

Ethylbenzene is another colorless liquid generally used in the production of styrenes, as a solvent and as a constituent of asphalt and naptha. It is also present in fuels such as gasoline and biomass derived gas. It has a characteristic sweet, gasoline-like odor

which can be detected at very low concentrations (1-2.3 ppm) (Department of Health and Human Services, 2007).

Ortho-xylene, meta-xylene, and para-xylene are part of the xylene group of aromatic solvents used in the oil industry for cleanup of surface pipelines, wellbore tubulars, and bore cleaning operations. The clear liquid with a sweet odor is used in place of benzene in many solvent applications due to benzene's health hazards but is also used in gasoline, phthalate plasticizers, polyester fiber, film, and fabricated items. It can also be formed in biomass gasification systems (Department of Health and Human Services, 2007).

These compounds are known to cause harm to humans, animals, and the environment. The human health and environmental hazards associated with each of these compounds is listed in Table 8 below.

*Table 8: Health Hazards of Volatile Hydrocarbons (Department of Health and Human Services, 2007)*

| Volatile Hydrocarbon | Health hazards | Environmental Effects |
|---|---|---|
| Benzene[1] | Known carcinogen (blood, blood system, other types of cancer); skin and eye irritant; harmful to nervous system; causes headache, nausea, drowsiness, confusion, severe lung damage, anemia; known mutagen | Highly flammable; high vapor density; water soluble; reacts violently with oxidizing agents |
| Toluene[2] | Irritant to eyes, nose, throat and skin; damage to liver and kidney through ingestion; depression of the central nervous system; causes fatigue, headache, confusion, weakness, muscular incoordination; female reproductive toxicity | Highly flammable; strong oxidizer; vapors may form explosive mixture with air; immiscible with water |
| Ethylbenzene | Throat irritation; chest constriction; neurological effects such as dizziness; central nervous system toxicity; damage to liver, kidney and eyes; causes headaches, dermatitis, narcosis, coma, cochlear impairment, edema | Highly flammable; sparingly soluble in water; due to high evaporation rate poses little to no significant environmental hazards |
| Xylenes | Irritant to eyes, skin, nose and throat; causes dizziness, excitement, drowsiness, incoordination, staggering gait, corneal vacuolization, dermatitis; targets central nervous system, gastrointestinal tract, blood, liver and kidneys | Flammability concerns; biodegradability; volatility leads to atmospheric contamination from contaminated water |

1. Bayliss et al. 1998.

2. Flowers et al., 2005.

As BTEX compounds have dangerous effects on both human health and the environment, concentrations of these compounds are regulated by various governmental organizations. In the United States, emissions limits are regulated by OSHA and

researched and recommended by NIOSH. OSHA sets enforceable permissible exposure limits (PEL) based on an 8-hour time-weighted average (TWA) in order to protect workers from the health hazards of a substance. There are standards for general industry as well as specific limits for shipyard employment and the construction industry. The short-term exposure limit (STEL) is the acceptable average exposure over a short time period, generally 15 minutes, as long as the time weighted average limit is not exceeded. NIOSH provides research, education and training for occupational health and safety and develops recommendations for the acceptable limits of concentrations of compounds in order to prevent work related injuries, illness, disability and death. The limits recommended by NIOSH for BTEX exposure are shown in Table 9.

*Table 9: Organic Hydrocarbon Permissible Exposure Limits (Department of Health and Human Services, 2007)*

| | **Time Weighted Average (TWA)** | **Short-term exposure limit (STEL)** | **Immediately Dangerous to Life or Health (IDHL)** |
|---|---|---|---|
| Benzene | 1ppm | 5ppm | 500ppm |
| Toluene | 100ppm | 150ppm | 500ppm |
| Ethylbenzene | 100ppm | 125ppm | 800ppm |
| Xylenes | 100ppm | 150ppm | 900ppm |

### 2.9. Producer Gas Combustion

Producer gas generated by air gasification of woodchips in a fixed bed downdraft gasifier has good heating value, making it a good fuel for combustion. Gasification reactors are able to convert the energy in solid biomass to energy in a gas at efficiencies up to 90%, depending on the reactor type and gasifying agent but the fuel must be used in

some additional process to provide useful energy. Hasler and Nussbaumer (1999) report lower heating values (LHV) of this type of producer gas in the range of 4.0-5.6MJ/$Nm^3$. The resulting fuel is generally used in gas stoves, turbines, boilers, or engines.

Turbines, however, have very low tolerance for particulate matter and alkalis suspended in the gas. Particles and metals can erode parts in the turbine system during operation, damaging the blades and reducing the useful life of the turbine (Kurz and Brun, 2001). Internal combustion (IC) engines can also be operated with producer gas derived from biomass. Both spark-ignited and diesel engines can run on biomass derived gaseous fuels but both have low tolerances for many of the contaminants in producer gas. Engine-quality gas must have very low concentrations of tars and particulate matter so that the engine is not subject to unnecessary corrosion and clogging. Tars entrained in the gas flow can condense in supply lines to the engine, in gas-air mixers, and on the intakes valves in the cylinders. Once the engine is allowed to cool after operation, tars collected on valves and valve stems harden and prevent valves from fully closing when the engine is restarted. Excess tars in the gaseous fuel can also clog filters leading to high pressure-drops and reduced overall efficiency of the system. The gas quality requirements for both IC engines and gas turbines are shown in Table 10.

*Table 10: Gas Quality Requirements (Hasler and Nussbaumer, 1999)*

| Contaminant | IC Engines | Gas Turbines |
|---|---|---|
| Particles ($mg/Nm^3$) | <50 | <30 |
| Particle Size (μm) | <10 | <5 |
| Tar ($mg/Nm^3$) | <100 | |
| Alkali Metals ($mg/Nm^3$) | | 0.24 |

The power output from an engine running on producer gas is dependent on the

heating value of the gas, ignition timing, and engine characteristics. IC engines must be modified for an appropriate air-fuel ratio and compression ratio for optimal operation when running on biomass derived gaseous fuels.

The emissions coming from the engine's exhaust are also important as this is the effluent emitted into the atmosphere. Federal regulations for a spark-ignited non-road engine are outlined in Title 40 of the Code of Federal Regulations (CFR) sections 1054.103 and 1054.105. The Phase 3 emissions standards for a Class II non-handheld engine apply to engines with a displacement greater than 250cc that was manufactured after 2008. This type of engine must have primary carbon monoxide emissions no greater than 610 g/kW-hr and a hydrocarbon plus NOx emissions less than 8.0 g/kW-hr. Compression ignited engine emission regulations for Tier 4 diesel engines are outlined in Title 40 CFR Section 1039. For the power output in the range of a small-scale gasification system, these regulations apply to engines manufactured after 2008. Emissions regulations for compression ignited and spark ignited engines are show in Table 11. Additionally, World Bank guidelines for stationary engine emissions are also shown in the following table.

*Table 11: Emissions Regulations*

| | **Tier 4 Compression Ignited Non-road Engine[1]** | **Phase 3 Spark Ignited Non-road Engine (Class II)[2]** | **World Bank Guidelines for Stationary Engines[3]** |
|---|---|---|---|
| CO (g/kW-hr) | 6.6 | 610 | - |
| HC+NOx (g/kW-hr) | - | 8 | - |
| NMHC+NOx (g/kW-hr) | 7.5 | - | - |
| PM (g/kW-hr) | 0.4 | - | 50 mg/$Nm^3$ |
| $SO_2$(g/ $Nm^3$) | - | - | 2 |
| NOx (g/ $Nm^3$) | - | - | 2 |

1. Code of Federal Regulations, title 40, sec. 1039.101, 2004
2. Code of Federal Regulations, title 40, sec. 1054. 103 and sec. 1054.105, 2008.
3. World Bank Group, 1998.

Other species of concern from biomass gasification emissions are organic solvents like the BTEX compounds. While the combustion of these aromatic compounds does not affect the efficiency of the engine and they are not currently regulated, they do pose a serious risk to the environment and human health. OSHA regulates the ambient concentrations of these hazardous hydrocarbons and it is necessary to monitor of the level of contamination in the immediate vicinity of biomass gasification system emissions.

# 3. Experimental Methods and Procedures

## 3.1. Introduction

A modified Imbert, downdraft fixed-bed reactor was part of the gasifier-generator system experimentally examined in this study. It produced the best combination of low tar and particulate matter concentrations, simple and stable operation, and good tolerance for a variety of feedstocks (Wei, 2005). All Power Labs donated the Power Pallet system to the University of Minnesota, Twin Cities for testing.

The skid mounted 10 kW system was equipped with a 3 cylinder, 962 cc Kubota natural gas head engine, Woodward L-series governor, and Mecc Alte generator. The system was instrumented with a Process Control Unit (PCU), thermocouples, flow meters, and pressure transducers. The PCU controlled the producer gas and air mixture entering the engine using a wide band Bosch oxygen sensor and shakes the ash grate as needed. Thermocouples measured temperature at the top and bottom of the reactor reduction, at the filter outlet, and at the inlet and outlet of each of the two heat exchangers. Mass air flow (MAF) meters measured the air-flow into the reactor and into the engine and an orifice flow meter measured the flow of producer gas from the filter to the engine. The pressure was measured at the bottom of the reactor, in the filter, at the engine inlet, at the combustion site, at the reactor inlet, and for the engine oil. Pine woodchips were selected for use in this study as they were easily obtained from local tree services in the size range, moisture content, and quantity needed. The gasifying agent was air and the system operated at atmospheric pressure. The determination of gaseous compounds, particulate matter, organic solvents, elemental carbon, and organic

compounds was carried out in two phases: sampling and analysis. The system specifications can be seen in Table 12 below.

*Table 12: Power Pallet Specifications (All Power Labs, 2013)*

| **Specifications** | |
|---|---|
| Power Output: | 1-10 kW |
| Engine: | Kubota 962cc spark fired 3 cylinder, natural gas |
| Generator: | Mecc Alte, 12 wire genhead 50 Hz or 60 Hz in single, split or 3-phase |
| Feed stocks: | Hard and soft woodchips, nut shells, coffee grounds, sawdust, corn cobs, manure, coconut shell and poultry litter |
| Feedstock Size: | 0.5-1.5 inches |
| Ash Content: | <5% |
| Fixed to Volatile Ratio: | >0.25 |
| Moisture Content (dry): | 10-30% (ideally <20%) |
| Feedstock Consumption: | 12 kg/hour at 10kW |
| Gas Flow Rate: | 5-27 $m^3$/hr |

The biomass feedstock, which was pine woodchips in this study, was stored in the hopper. A feed auger moved the woodchips from the hopper to the reactor through a section of pipe that was first heated by producer gas leaving the reactor in a heat exchanger configuration and then heated by engine exhaust in a second heat exchanger as the biomass entered the reactor. The much dryer biomass then underwent the thermochemical conversion in the reactor necessary to generate producer gas. The ash fell through the grate at the bottom of the reactor and the producer gas left the reactor at the bottom. The very hot producer gas entered the heat exchanger in the feed auger for biomass from the hopper where the gas was cooled. The producer gas then entered a cyclone where much of the particulate matter was removed followed by the packed bed filter, filled with sawdust, woodchips, and foam. The packed bed filter was able to reduce

the concentrations of many of the contaminants by cooling the gas stream below the dew point of the gaseous contaminants. During startup, all the producer gas was diverted away from the engine and allowed to burn with atmospheric air in the flare. Once operation was stable at appropriate temperatures, pressures, and quality, the producer gas was combusted with air in the spark-ignited engine powering the generator. Engine exhaust was then passed through the heat exchange at the biomass feed auger to preheat the biomass leaving the hopper and the engine emissions were to the environment. The generator's electrical load was varied with electrical resistance heaters which consumed 1.5kW each. Three heaters were used to determine the effect of electrical loading, varying from 0 kW to 4.5 kW, on many of the system's properties and emissions. For most experiments, gas was sampled from three locations: before the packed bed filter after the cyclone, after the packed bed filter and after the engine. Figure 7 shows the general flow of solids and gases in the system and the locations of the three sampling points.

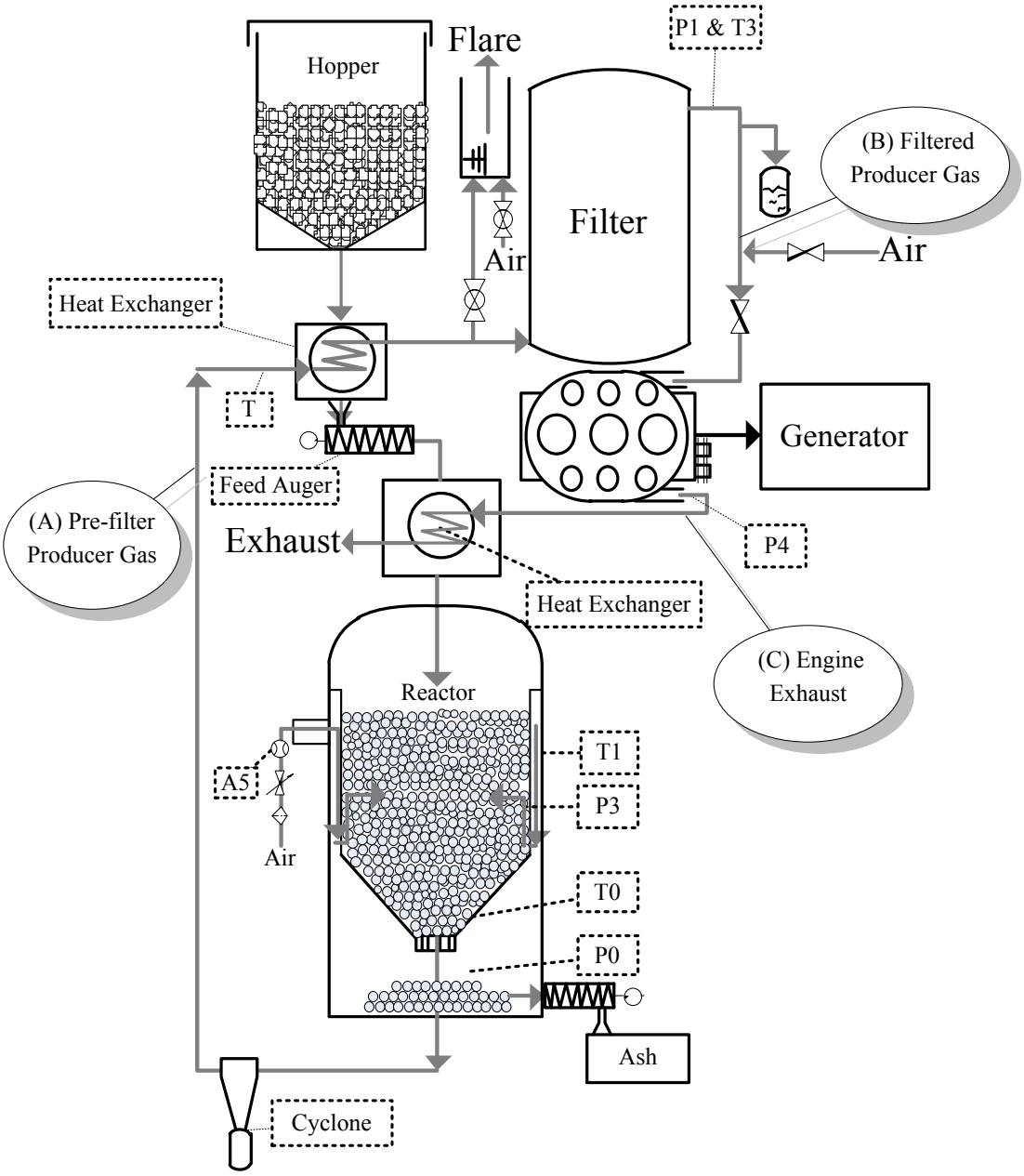


*Figure 7: Power Pallet® Schematic (All Power Labs, 2013)*

## 3.2. Experimental Setup and Methods

### 3.2.1. Moisture Analysis

Moisture content in the feedstock fluctuated depending on the supplier's available pine woodchips and weather conditions. To eliminate extrinsic moisture from the feedstock, woodchips were air-dried prior to loading into the feedstock hopper. The moisture content of the woodchip feedstock was measured after the air-drying, prior to each test cycle. Approximately 1 kg of woodchips was sampled from the hopper, placed in a seal plastic bag and weighed using a Mettler PB3000 balance. The feedstock sample was then placed on baking sheets and cooked in an American Scientific Products DP-31 Vacuum Oven at 105°C±2°C for 24 hours. Samples were allowed to cool in a dry, temperature-controlled environment and then reweighed. Moisture content was determined on a dry basis using the following equation:

$$MC_{dry} = \frac{m_{wet} - m_{dry}}{m_{dry}} \times 100$$

### 3.2.2. Ramen Laser Scattering Analysis

Ramen Laser Scattering was used to determine the volumetric concentrations of major gases in the producer gas and in the engine exhaust. Ramen Laser Scattering uses the unique scattering of monochromatic light as it passes through a substance to determine the concentrations of each gas in the mixture. The detector module shines a low-powered laser through the gas-settling chamber and optical filters and sensors for each of the compounds to be measured determine the intensity of light scattering at its

specific frequency (Biedrzycki, 2011). In the Atmospheric Recovery, Inc.'s (ARI) Ramen Laser Gas Analyzer (RLGA), a specially designed computer logs and interprets the digital signals, giving real-time gas composition for eight gases: $O_2$, $N_2$, $H_2O$, $H_2$, $NO_2$, CO, $CO_2$ and $C_xH_y$. Figure 8 shows the gas settling chamber and the eight optical sensing ports.

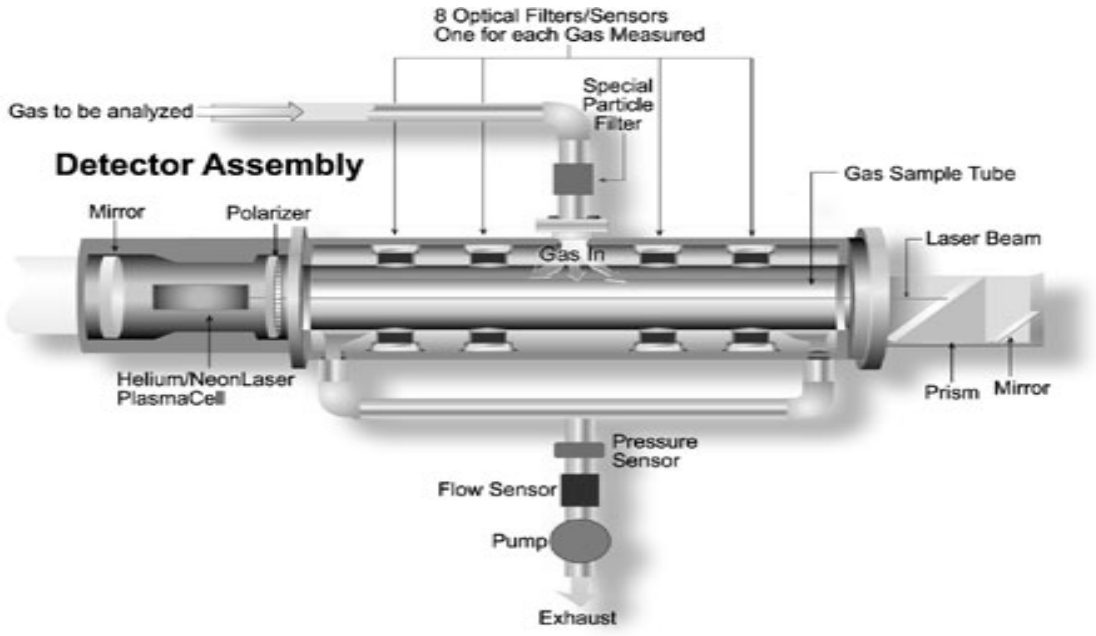


*Figure 8: Detector Module (Atmospheric Recovery, Inc., 2010)*

Gas was sampled on-line from the gasifier at two sampling locations: after the packed bed filter and after the engine. Gases were not sampled before the packed bed filter as the concentration of contaminants in the gas were too high for the RLGA and it was assumed that the gas composition of major gaseous species did not change through

the inert, packed bed filter. The major advantage of using on-line gas composition monitoring was the ability to ensure that gasifier conditions remained stable over long periods of testing as well as over multiple days of testing despite small changes in feedstock and operating conditions. Additionally, the comparison of producer gas composition and engine exhaust composition gave an understanding of combustion efficiency within the engine. The sampling procedure was the same at both sampling locations.

Sampling was performed using a diaphragm gas pump with a 1 L/min orifice. Gas was dried using a glass bead dryer submerged in an ice bath and the gas then passed through a fibrous in-line filter. A second filter was used on the inlet of the gas analyzer to protect the instrument from particulate matter. The second filter was an ARI, Inc. gas filter with 0.2 μm pores. The gas was sampled at approximately 300 mL/min into the RLGA throughout all tests and the location of gas sampled was varied throughout each test to ensure stable producer gas and engine exhaust compositions. The same sampling setup was used in both sampling location and can be seen in Figure 9.

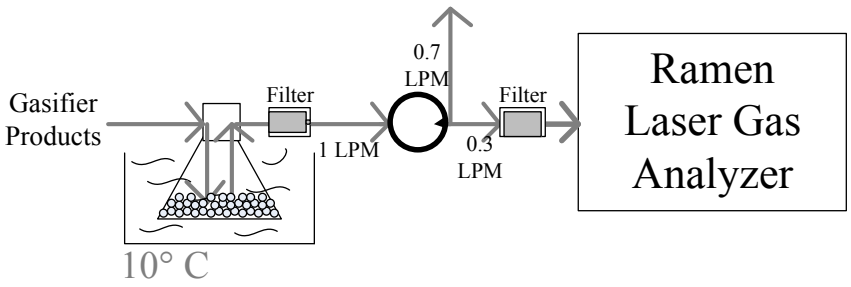


*Figure 9: Ramen Laser Gas Analysis Setup*

### 3.2.3. Micro-GC Analysis

An Agilent Micro-GC 490 with two columns was used for the analysis of volatile hydrocarbons. The Micro-GC was configured for use with ultra-high purity (UHP) Helium as the carrier gas (>99.999% He). The two columns used with the Micro-GC were PloraPLOT Q and CP-Sil 8 CB. The PloraPlot Q channel used a non-polar, porous fused silica coated column to distinguish hydrocarbons ($C_1$-$C_6$), halocarbons/freons, anesthesia gases, $H_2S$, $CO_2$, $SO_2$, and volatile solvents. The CP-Sil 8 CB channel used a low-polarity, fused silica column to separate hydrocarbons ($C_3$-$C_{10}$), aromatics and organic solvents. A method was developed for each column to allow for proper peak differentiation and recognition with short sampling times for all of the compounds of interest. The columns were calibrated using four calibration gases at varying levels of dilution to achieve approximately linear calibration curves for nitrogen, carbon dioxide, methane, ethane, propane, butane, pentane, hexane, benzene, toluene, ethylbenzene, m- and p- xylene, and o-xylene. The Micro-GC method, calibration gas data, and calibration curves can be found in Appendix B.

Gas samples were taken at three locations of the gasification system: after the cyclone before the packed bed filter, after the packed bed filter, and from the engine exhaust. Samples were drawn from the system using stainless steel ¼" heated lines at 191°C±11°C. The gas sample then entered a heated particulate matter filter from Unique Heated Products maintained at 191°C±11°C with a fibrous filter element. Gas then entered a 250 mg Tenax® TA sorbent tube maintained at 80°C±2°C. The Tenax® TA removed hydrocarbons heavier than the Micro-GC detectable limit, tars, and moisture

from the gas sample to protect the sensitive columns in the Micro-GC. The temperature was chosen so that Micro-GC detectable aromatic solvents (up to xylenes) passed through the sorbent tube due to their low breakthrough volume at the specified temperature.

Clean and empty 5L Tedlar® gas sampling bags were pre-filled with 500 mL UHP helium prior to gas sampling. This dilution was necessary for preventing drop out of gases compounds of interest in the sampling bags. The gas to be tested was sampled at a flow rate of 250 mL/min for 5 minutes. The long sampling time was necessary to obtain a representative average gas composition at each of the sampling locations and generator loadings and eliminate instantaneous fluctuations in the gas composition. The bag samples were further diluted with 500 mL UHP helium after the gas was sampled from the gasifier system to ensure that all compounds of interest were fully eluted from the sorbent tube and sampling lines.

Gas samples were immediately analyzed with the Micro-GC after sampling. Gas samples were drawn from the Tedlar® sampling bags using the Micro-GC's built-in pump. The gas samples passed through a Genie® membrane filter to further protect the sensitive columns of the Micro-GC from moisture and particulate matter. After the membrane filter, gas entered a heated sample inlet line at 100°C. The gas samples were analyzed using the method developed specifically for the gasifier project using OpenLAB EZChrome®. Each bag sample was processed through the Micro-GC three times and every run was analyzed to ensure consistent results. Plating of BTEX compounds onto the Tedlar® bags can occur after gas settles for a short time, so sampling was done as soon as possible with as little time as possible between each of sample's three runs.

Atmospheric air was sampled through the Micro-GC between each change in gas sampling location and/or generator loading condition to ensure that all compounds were fully eluted from GC columns and there was no contamination between samples. Furthermore, sampling air from between each test ensured that the Micro-GC's operation was stable with no drifting baseline.

### 3.2.4. Particulate Matter Analysis

#### 3.2.4.1. Inertial Impaction Separation

Samples were taken at three sampling locations for size selective, gravimetric particulate matter analysis: raw producer gas after the cyclone before the packed bed filter, filtered producer gas after the packed bed filter, and from the engine's exhaust. A Bureau of Mines four-nozzle, single stage impactor was used to determine the gravimetric concentrations of particulate matter above the primary cut size of 0.8 μm. For a Bureau of Mines impactor operated with a flow rate of 2 liters/minute (LPM) and gravimetric analysis within 0.1 mg, the 0.8 μm aerosol concentrations is estimated to have a priori limit of detection of 0.3 $mg/m^3$ (Cantrell and Rubow, 1999). The impactor was used with 37 mm substrates prepared from 0.0254 mm thick aluminum foil with 99.5% metals base purity. A center hole 3/8" in diameter was made in the middle of the foil disk to allow gas samples to exit the impactor. A 1" diameter Zeflour® rings with a 25 mm diameter center hole was attached using superglue to the center of each of the substrates. The Zeflour® had pore size of 2μm and PTFE support.

A filter downstream of the impactor was used to obtain gravimetric measurements

of particulate matter with aerodynamic diameter less than 0.8μm. The Whatman PTFE membrane filters were 25mm in diameter with 0.2μm pore size and polypropylene grid support. These membrane filters are chemically stable, inert, and can be used at temperatures up to 120°C. PTFE membrane filters have good structural integrity even at elevated temperatures unlike quartz filters.

Each impactor substrate and filter was prebaked to remove volatile material from the surface and eliminate atmospheric moisture from the surfaces. The substrates and filters were baked at 80°C±1°C for 5 hours, weighed, and baked again for increments of 1 hour until the mass was stable within ±3 μg. Substrates were loaded into individual 47mm Pall Analyslides to avoid contamination and moisture accumulation on the substrates. Furthermore, gloves were worn during preparation and handling of substrates and filters to further reduce the chance of contamination. Filters and substrates were weighed using a Cahn Micro-Balance C-31 with range of 0-250mg and accuracy of 1μg in a temperature and humidity controlled environment (25°C and 30% RH).

Gas samples were drawn from the gasifier system using a particulate matter sampling probe inserted into the gas stream and a diaphragm gas pump. Isokinetic sampling was not used, as it is not necessary for submicron particles measured with inertial impaction (Kittleson et al., 1999). The ¼" stainless steel sampling lines were heated to 191°C±5°C and the impactor and filter setup was maintained at 80°C±5°C to prevent condensation of any moisture from the gas samples on the substrates or filters. Two impactor and filter setups were run in parallel in the same heated sampling box to maximize data collection. The sample line was split to accommodate the two sampling

trains and the lines were rejoined after the impactors and filters before the pump. The flow was maintained at 2 LPM for each arm of the sampling setup, with a total flow rate of approximately 4 LPM from the system through the pump. Maintaining a flow rate of 2 LPM for each of the sampling lines was essential to keep the cut size constant.

Flow was adjusted using a rotameter with valve fitting and calibrated using a Gilibrator with a standard flow cell (20 cc/min-6 LPM). Flow rate and sampling time was recorded for each sample. Each impactor and filter sampling train was connected to one another using stainless steel barbed fittings and non-conductive tubing. The impactors and filters were oriented vertically to reduce losses of large particles due to settling in the impactor, filter holder or tubing. The sampling setup can be seen in Figure 10 and Table 13 shows the flow rates and sampling times used for each of the three sampling locations.

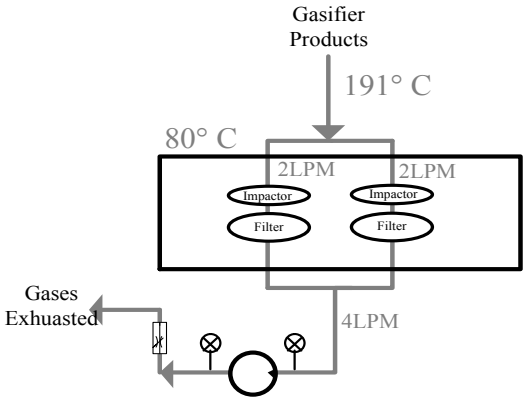


*Figure 10: Size Selective PM Mass Sampling Setup*

*Table 13: Size Selective PM Mass Sampling Flows and Sampling Times*

| | Flow Rate (LPM) | Sampling Time (min) |
|---|---|---|
| Pre-filter | 2 | 20 |
| Post-filter | 2 | 50 |
| Engine Exhaust | 2 | 50 |

Sampling time was adjusted for the different sampling locations to ensure that impactor substrates and filter media were not overloaded with particles but also to ensure that there was adequate particulate matter deposition to ensure accurate mass

measurements. Gas was sampled from the pre-filter raw producer gas location for 20 minutes at 2 LPM for a total gas volume of 40 L through each of the two impactor and filter setups. In the other two sampling locations, after the packed bed filter and at the engine's exhaust, samples were taken for 50 minutes at 2 LPM so that 100 L of gas was sampled in each of the sampling trains. A longer sampling time was necessary to have adequate mass accumulation at the locations with very low PM concentrations. Impactor holders filter holders, fittings, and connections were cleaned between each sampling location and/or generator loading condition using isopropyl alcohol and dry, dust-free, compressed air.

Loaded substrates and filters were transported after sampling in individual 47 mm Pall Analyslides and were weighed using the Cahn microbalance C-31 as soon as possible to eliminate contamination, particularly from atmospheric moisture. Particulate matter concentrations were analyzed by determining the average mass accumulation for each loading condition at each sampling location over various days of testing normalized for the specific flow rate and sampling time of each test. Average concentrations were found in units of $\mu g/cm^3$ and the margin of error was determined using statistical propagation of errors.

#### 3.2.4.2. Total Mass Concentrations

Total mass concentrations were taken at the same three sampling locations as the size-selective PM analysis to verify the results. 25mm Whatman PTFE membrane filters with 0.2 μm pore size with polypropylene backing were used to collect all particulate

matter regardless of particle sizes from the gas stream for gravimetric analysis. Filters were prebaked at 80°C±1°C until their masses were stable within ±3 μg, pre-weighed, and transported in individual 47 mm Pall Analyslides.

The ¼" stainless steel sampling lines were heated to 191°C±5°C and two filters were run in parallel using a common sampling line from the system. The sampling line was rejoined before the diaphragm pump and the flow was assumed to be equal in each sampling train. Filters holders were placed in the sampling setup vertically to reduce loss of large particles due to gravitational settling the holder or sample lines. During sampling, filters in stainless steel filter holders were heated to 80°C±5°C to ensure there was no condensation in the holders or on the filter media. The flow rate was set to 4 LPM through each branch of the sampling train for a total flow of 8 LPM through the pump. The flow was set using a rotameter with a ball valve and calibrated using a Gilibrator with a high flow cell (2 to 30 LPM).

Sampling time was adjusted for the different sampling locations, as it was necessary to accumulate sufficient particulate matter for gravimetric analysis without overloading the filter media, which would lead to PM losses when handling the filters. The sampling setup used for total particulate mass measurements is shown in the following diagram.

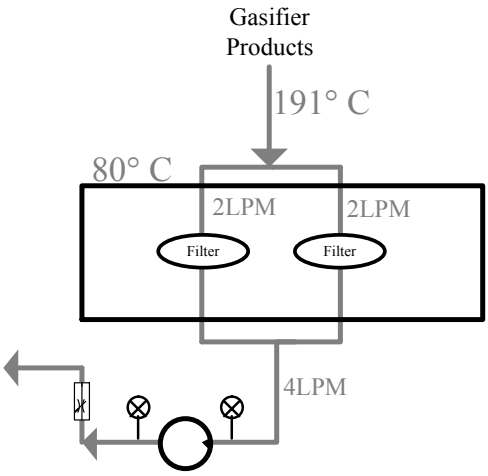


*Table 14: Total PM Mass Sampling Flows and Sampling Times*

| | Flow Rate (LPM) | Sampling Time (min) |
|---|---|---|
| Pre-filter | 4 | 5 |
| Post-filter | 4 | 30 |
| Engine Exhaust | 4 | 30 |

*Figure 11: Total PM Mass Sampling Setup*

Samples were taken for 5 minutes for the raw, unfiltered producer gas and for 20 minutes for the filtered producer gas and for the engine exhaust. Filters were transported in individual 47mm Pall Analyslides and weighed as soon as possible using the Cahn microbalance C-31. Analysis of total PM concentrations was performed by normalizing all measured masses of PM over the tare mass of the filter to take into account the flow rate and time sampled to find concentrations in units of $\mu g/cm^3$.

### 3.2.5. Elemental carbon and organic carbon analysis

Elemental carbon (EC) and organic carbon (OC) measurements were taken using the thermal optical analysis method outlined in NIOSH 5040 for diesel particulate matter. Gases were sampled at the three sampling locations: before the packed bed filter, after the packed bed filter and at the engine exhaust. Gas sampling was done using ¼" stainless steel heated sample lines at 191°C±1°C and filters were maintained at 80°C±1°C for the

duration of sampling to reduce condensation on the filter's surface. The 37mm quartz filters were pre-cleaned in a low temperature asher for 2 to 3 hours or in a muffle furnace for 1 to 2 hours at approximately 800°C before being placed in a 3-piece 37mm cassette with cellulose support pad. Filters were prepared and sealed by SKC, Inc. (Birch and Cary, 1996).

For pre-filtered, raw producer gas, a size selective impactor was used before the quartz filter, as the extremely high concentrations of soot would overload filters before sufficient organic carbon could accumulate. The Bureau of Mines impactor with aluminum foil substrate and Zeflour® ring was connected to the 3-piece cassette using stainless steel fittings and non-conductive tubing. Gas was sampled at a flow rate of 0.3 LPM for the pre-filtered producer gas due to high concentrations of particulate matter. As the flow rate was not the standard 2 LPM for this impactor, the aerodynamic cut size was not 0.8 μm. The flow rate was reduced as the quartz filters, even with the addition of the PM impactor, could be overloaded very quickly at higher flow rates. Furthermore, the PM could deposit in peaks in the center of the filter at high flow rates rather than uniformly across the filter's entire exposed surface. For the sampling locations with lower concentrations of particulate matter, such as after the packed bed filter and from the engine's exhaust, the inertial impactor was not used and a flow rate of 2 LPM was used. Additionally, the sampling time was increased to allow for adequate deposition on the filter.

A non-isokinetic particulate matter sampling probe and diaphragm pump were used to sample gases from the system. The flow was set with a rotameter with a ball

value and calibrated using a Gilibrator with a standard flow cell. The cassettes containing the quartz filters were kept sealed until they were ready for sampling and immediately frozen after sampling until analysis. For each of the three sampling locations, one filter cassette was loaded with two filters to determine if there was additional EC and/or OC which was able to penetrate the first filter. These "doubles" were loaded into the cassettes and resealed in a temperature and humidity controlled environment using clean tools. The sampling setup was the same for these double filter cassettes as with the single filter samples. The sampling setup for the EC and OC analysis is shown in the following diagram.

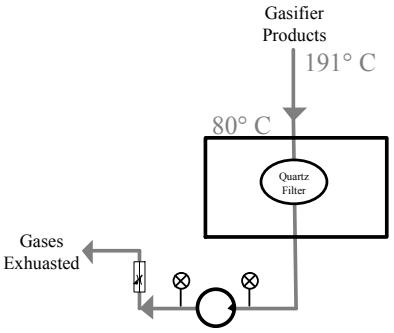


*Figure 12: EC/OC Sampling Setup*

*Table 15: EC/OC Analysis Sampling Flows and Times*

| | Flow Rate (LPM) | Sampling Time (min) |
|---|---|---|
| Pre-filter | 0.3 | 5 |
| Post-filter | 2 | 60 |
| Engine Exhaust | 2 | 60 |

Samples were analyzed at the University of Wisconsin's Industrial Hygiene Laboratory using evolved gas analysis by thermal-optical analyzer. Using a 1 $cm^2$ punch from the loaded filter, the concentrations of elemental carbon and organic carbon were determined in units of $\mu g/cm^2$. In the case of pre-filtered producer gas, where a size selective impactor was used before the quartz filter, it was assumed that all particulate matter that accumulated on the impactor substrate during sampling was elemental carbon,

as fly ash and soot are a major contaminant in untreated producer gas. Blank filters were also analyzed using the EC/OC method to determine the baseline measure of carbon on unused filters taken to the sampling site but not used (Birch and Cary, 1996).

### 3.2.6. Test Matrix

The following table shows the tests that were performed at each sampling location and at each generator loading condition. Portable resistance heaters were used to apply the generator loading for the varied generator-loading conditions between 1500 W and 4500 W. The electrical current was measured during all tests to ensure steady electrical loading. RLGA Gas Analysis was not performed on pre-filtered producer gas as the level of contamination in the gas from contaminants could damage sensitive parts in the instrument. Furthermore, it is assumed that the concentrations of each of the eight gases measured by the RLGA would not change as the producer gas was cleaned up in the packed bed filter.

*Table 16: Test Matrix*

| Sampling Locations | Load (W) | RLGA Gas Analysis | Micro GC Analysis | Impactor and Filter PM Analysis | Total PM Analysis | EC/OC Analysis |
|---|---|---|---|---|---|---|
| (A) Pre-filter Producer Gas | 1500 | × | ✓ | ✓ | ✓ | ✓ |
| | 3000 | × | ✓ | ✓ | ✓ | ✓ |
| | 4500 | × | ✓ | ✓ | ✓ | ✓ |
| (B) Filtered Producer Gas | 1500 | ✓ | ✓ | ✓ | ✓ | ✓ |
| | 3000 | ✓ | ✓ | ✓ | ✓ | ✓ |
| | 4500 | ✓ | ✓ | ✓ | ✓ | ✓ |
| (C) Engine Exhaust | 1500 | ✓ | ✓ | ✓ | ✓ | ✓ |
| | 3000 | ✓ | ✓ | ✓ | ✓ | ✓ |
| | 4500 | ✓ | ✓ | ✓ | ✓ | ✓ |

## 3.3. Experimental Analysis

### 3.3.1. Gas Analysis

In order to perform a full energy balance of the gasifier system, some of the flows of gases and solids in the system that were not measured had to be determined through mass balances. The missing flows that had to be calculated were the mass flow rate of woodchips into the reactor and the mass flow rate of the dry producer gas into the engine after moisture had been dropped out.

The following procedure was used for determining the dry producer gas flow rate from the gas yields and generator loading conditions using a nitrogen balance in the reactor. As woodchips were used as the feedstock, it was assumed that there was essentially no nitrogen present in the system except from the air added as the gasifying agent in the reactor and the air that aspirates the engine. This procedure also assumed that the gasifier was operating at stable conditions, that the producer gas composition was

known, and that the mass flow rates of the moist producer gas, the air into the reactor, and the air into the engine were known. This calculation assumes that 76% of the air entering the reactor was nitrogen. The subscript "dry" represents the dry producer gas after moisture had been removed.

$$\dot{m}_{dry} = \frac{\dot{m}_{N_2} \times MW_{dry}}{\%N_2 \times MW_{N_2}} = \frac{0.76 \times \dot{m}_{Reactor\ Air} \times MW_{dry}}{\%N_2 \times MW_{N_2}}$$

The mass flow rate of woodchips through the reactor was also computed at each of the loading conditions. In order to perform the mass balance, it was assumed that the pine woodchips had approximately 1.12% ash content (Toms and Lewis, 1987). Some of this ash was removed from the reactor through the ash auger as it settled through the grate at the bottom of the reactor. The remaining ash became entrained in the gas stream but was mostly removed in the particle cyclone and in the packed bed filter. Therefore, it was assumed that wood ash was fully removed from the gas stream before the flow rate of the moist producer gas was measured using the orifice flow measurement. The calculation for wood flow rate was performed using a mass balance for all flows of material into and out of the reactor and the final calculation was as follows.

$$\dot{m}_{wood} = \frac{\dot{m}_{wet\ producer\ gas} - \dot{m}_{Reactor\ Air}}{0.9888}$$

The molecular weight of the dry producer gas was computed using the known concentrations of the eight major gas compounds present in the producer gas, found with

the Ramen Laser Gas Analyzer after moisture had been removed, and the molecular weight of each of the gas compounds.

$$MW_{dry} = \sum_{i=1}^{8} \%x_i \times MW_i$$

The lower heating value (LHV) of the producer gas was calculated at each of the generator loading conditions, too. The LHV was determined using the gas concentrations of the combustible gas compounds present in the producer gas, as measured by the Ramen Laser Gas Analyzer and the LHV of each of the combustible gas compounds. The following equation was used for this computation.

$$LHV_{PG} = \%H_2 \times LHV_{H_2} + \%CH_4 \times LHV_{CH_4} + \%CO \times LHV_{CO}$$

### 3.3.2. Gasification Efficiency Analysis

In order to better understand the system's ability to convert biomass into useful energy, the efficiency was determined at various points throughout the system. The cold gas efficiency was defined as the efficiency of the reactor to convert energy in the biomass to bond energy in the producer gas and was referred to as the efficiency of the reactor. The reactor efficiency was computed using the following equation:

$$\eta_{Reactor} = \frac{LHV_{PG} \times \dot{m}_{PG}}{LHV_B \times \dot{m}_B}$$

Where,

$LHV_{PG}$ is the lower heating value of the producer gas $\left(\frac{kJ}{kg}\right)$

$\dot{m}_{PG}$ is the mass flow rate of the dry producer gas $(\frac{kg}{s})$

$LHV_B$ is the lower heating value of the biomass $(\frac{kJ}{kg})$

$\dot{m}_B$ is the mass flow rate of the biomass $(\frac{kg}{s})$

The ability of the electrical generator to convert energy in the bonds of the producer gas to electrical energy was defined by the following equation:

$$\eta_{Engine/Generator} = \frac{\text{Electrical Output}}{LHV_{PG} \times \dot{m}_{PG}}$$

The overall system efficiency was defined as the system's ability to convert energy bound in the solid biomass to electrical energy from the generator. The overall efficiency was calculated using the following equation:

$$\eta_{System} = \frac{\text{Electrical Output}}{LHV_B \times \dot{m}_B}$$

## 4. Results and Discussion

The objectives of this research were to quantify many of the contaminants in producer gas generated from a small-scale biomass gasifier system, understand the engine's ability to cleanup contaminants, and to evaluate the energy balance of the overall system. A comprehensive sampling setup was developed for the study to accurately and consistently sample gas and contaminants from the system using portable and versatile instruments. Emissions and efficiency data were collected from experiments at three different generator load settings for the 10kW system. Generator loading was varied from 1500W to 4500W for the 10kW system.

There was significant experimental error in tests at 3000 W. Current fluctuated by over 20% when the loading was 3000 W while the current fluctuated less than 5% for both 1500W and 4500W tests. The flow rate of producer gas into the engine and the mass air flow into the engine fluctuated by approximately 15% for tests at 3000 W while fluctuations in the same flows at other generator loads was about 5%. This suggests that the governor was not properly tuned at this frequency leading to high experimental errors for the 3000W loading condition.

### 4.1. Effect of Electrical Loading on Gas Compositions and System Efficiency

Producer gas composition was measured after the packed bed filter and after the engine using the Ramen Laser Gas Analyzer (RLGA). Figure 13 and Figure 14 show the composition of the major gaseous species in the filtered producer gas and in the engine exhaust gas for the three generator loading conditions. The gas concentrations are plotted

on a log scale, as there was a wide range of concentrations for the various gases. For example, nitrogen ($N_2$) can account for up to 45% of the producer gas and 77% of the engine exhaust while oxygen ($O_2$) concentrations are approximately 1% of both the producer gas and the engine exhaust. The total moisture was not measured in either the producer gas or engine exhaust as most of the entrained moisture was removed prior to sampling with a glass bean dryer and ice bath. It was not possible to measure the total moisture in either of the gas samples because of the moisture limit of the RLGA. As a result, concentrations shown in the following figures are on a semi-dry basis.

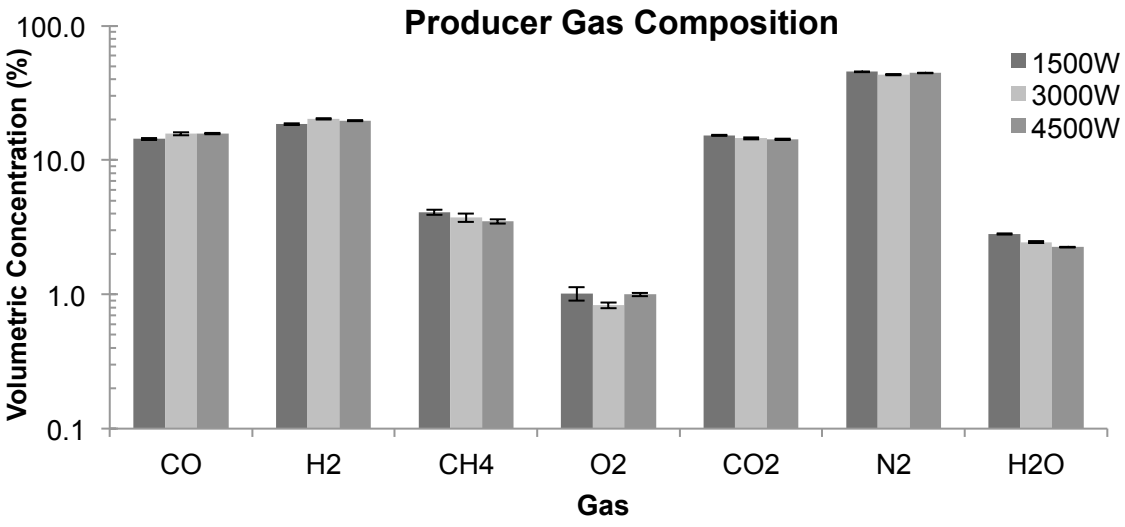


*Figure 13: Producer Gas Composition for Different Generator Loading Conditions*

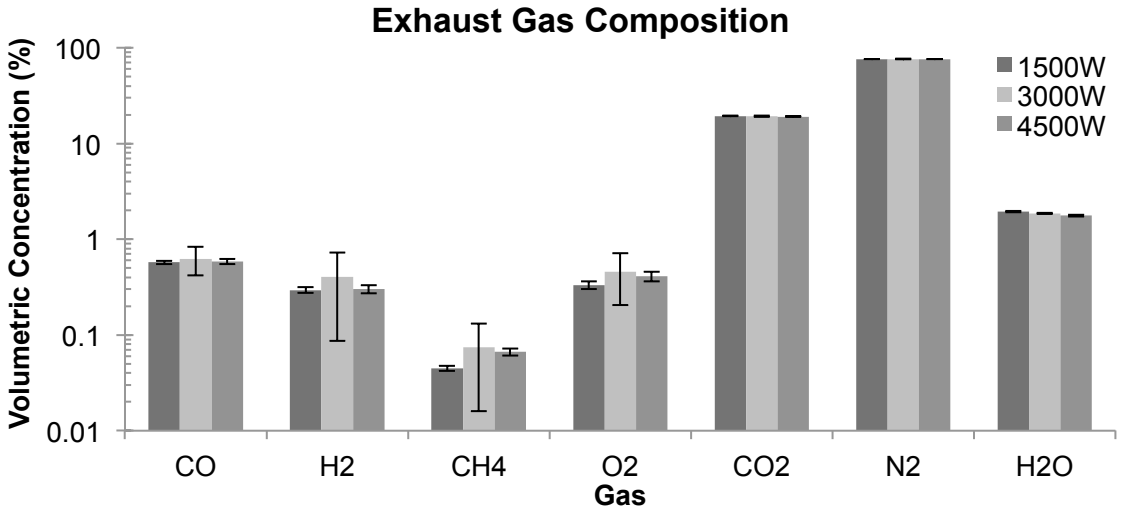


*Figure 14: Exhaust Gas Composition for Different Generator Loading Conditions*

The composition of the producer gas measured in this study confirms results by Hasler and Nussbaumer (1999) and Zainal et al. (2001) who measured and modeled producer gas from fixed bed downdraft gasifiers operating with wood chips. The reported values of CO and $H_2$ are in line with previous studies with approximately 17% CO and approximately 20% $H_2$ in the producer gas. The producer gas from the downdraft reactor, operating with pine woodchips and air as the oxidizing agent was calculated to have a lower heating value (LHV) of approximately 6 $MJ/Nm^3$ which is in line with results found by Hasler and Nussbaumer (1999) who predict LHVs for producer gas from this type of gasifier up to 5.6 $MJ/Nm^3$.

Figures 13 and 14 show that measured gas concentrations were constant as a function of generator load for both engine exhaust and producer gas. This suggests that the gasifier was sized sufficiently to meet the higher fuel demands needed for higher generator loads. It would be expected that if the producer gas rate required was too high,

the concentrations of $H_2$ and CO would be reduced. However, it was found that the system was able to adapt quickly and consistently to changing generator loads by increasing biomass flow into the reactor, increasing air flow into the reactor, and increasing air flow into the engine to maintain stable operation.

Concentrations of combustible gases were used to determine the heating value of the biomass derived producer gas. The concentrations of the major combustible gas species in the producer gas, namely methane ($CH_4$), carbon monoxide (CO), and hydrogen ($H_2$) were very stable over the range of generator-loading conditions tested. The conversion of these combustible compounds in the engine was very high, indicating that the engine was producing complete combustion regardless of the generator load. The combustible compounds were consumed by the engine with concentration reductions of 96% for CO and 98% for both $CH_4$ and $H_2$. The total concentration of combustible species remaining in the engine exhaust gas was less than 1% of the total gas. Figure 15 shows the concentrations of combustible compounds in the producer gas and in the engine exhaust plotted on a log scale to show the vastly different concentrations of combustible gases in the producer gas and engine exhaust. As the calculated lower heating value (LHV) of the producer gas is entirely dependent on the three major combustible gases, it is also shown for each generator loading condition.

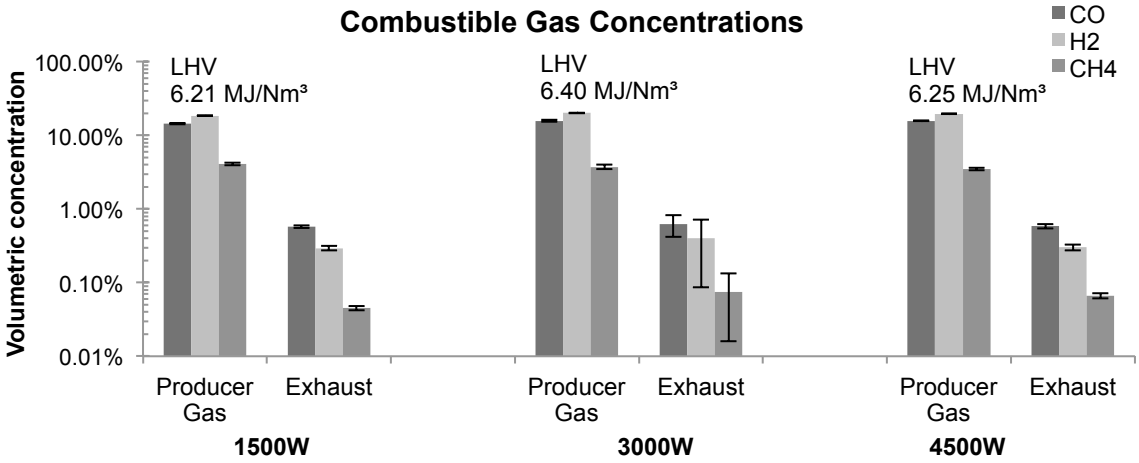


*Figure 15: Combustible Gas Conversion in the Engine*

The efficiency of the gasifier, engine, and overall system were calculated at the various generator loading conditions using the gas analysis methods previously described. These results are shown in Figure 16. Reactor efficiency increased significantly with increasing electrical load. As generator loading increased, more producer gas was required and therefore more biomass was gasified in the reactor. With these higher throughputs of producer gas in the constant temperature reactor and the constant heat loss from the system, the heat loss was a less significant portion of the power output and therefore the efficiency of the reactor and overall system increased. The engine however had mostly constant efficiency as a function of load to the statistical significance of the testing with mean efficiency varying between 11% and 16%. The fuel, having constant gas composition as was seen by the RLGA measurements, has a constant ratio of specific heats and the engine had a constant compression ratio. As a result the engine efficiency remained constant. Although the engine efficiency would be expected to increase with higher output, tests in this work were over a very small range of

generator loads and did not show significant increases in efficiency. Additionally, the air fuel ratio in the engine was stable for most of the generator loading conditions. As the flow rate of producer gas increased for higher generator loads as did the flow rate of air into the engine, adjusted automatically by the governor to maintain complete combustion in the lean burning engine. The engine and generator are oversized for the demands of this study and the limits of the system were not challenged.

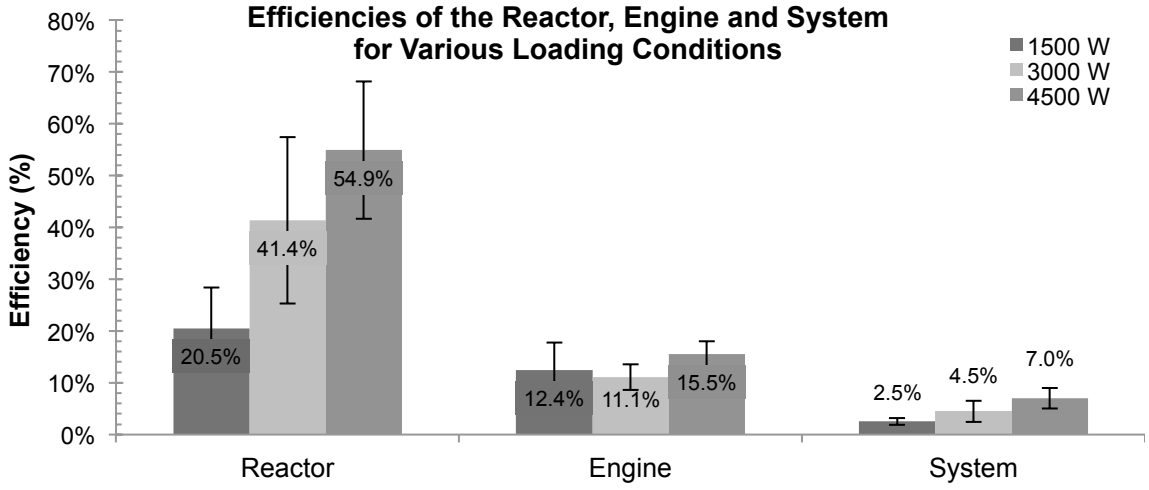


*Figure 16: Efficiencies for the Reactor, Engine and System for Various Loading Conditions*

### 4.2. Effect of Electrical Loading on Contaminants in the System

One of the major concerns in using gasification for distributed energy generation is the high concentration of harmful contaminants present in the producer gas and the expectation that these would be emitted from the overall generator system. The level of particulate and BTEX contaminants emitted from the small-scale biomass gasifier-generator was measured for various generator loading conditions. The central goal was to

determine the ability of the producer gas filter and the engine to reduce such contaminants to low levels before exhaust enters the environment.

### 4.2.1. Particulate Matter

The particulate matter (PM) emissions were measured at three sampling locations within the system. PM was measured in two size ranges: above and below 0.8 μm. Figure 17 shows the mass concentrations of both large PM (>0.8 μm) and small PM (<0.8 μm) at various locations within the gasification system under different generator loading conditions on a log scale. PM concentrations were stable over the range of generator loadings applied, suggesting that PM production is independent of generator loading. All PM concentrations were significantly reduced through the packed bed sawdust filter yet PM concentrations for both large and small PM was stable through the engine. The measured level of contamination of PM before the packed bed filter but after the cyclone in this system was in line with results by Hasler and Nussbaumer (1998) who found bimodal size distribution by weight for a wood bark mixture.

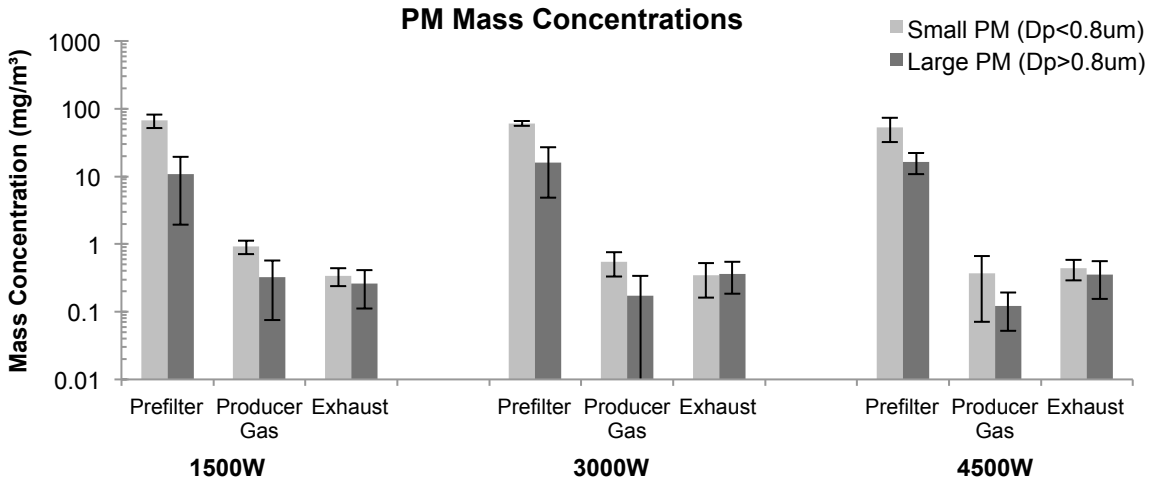


*Figure 17: PM Concentrations at Various Generator Loading Conditions*

The packed bed filter was able to largely eliminate PM contaminants in the producer gas from the gasifier. The concentrations of both small and large particulate matter were reduced by over 96% for all generator-loading conditions in the filter. This confirms the work of Hasler and Nussbaumer (1999) which measured PM removal efficiency in a sand packed bed filter at 70-99%. The packed bed filter was able to reduce small particles (<0.8 μm) by 98-99.3% and large particles (>0.8 μm) by 97-99.2%.

While the packed bed filter is able to largely eliminate most of contamination from PM, there is still approximately 1 mg/Nm$^3$ of particles entering the spark ignited engine. This low level of contamination by PM is not harmful to components in the engine. Hasler and Nussbaumer (1999) report that IC engines require PM mass concentrations less than 50 mg/Nm$^3$. The engine, however, was not able to significantly reduce total PM concentrations during combustion and mass concentrations of total PM were similar before and after the engine. Total concentrations of PM remained stable

through the engine although the size distribution changed in some tests. The total PM concentrations from the engine's exhaust were approximately 0.6-0.8 mg/$Nm^3$.

Some of the contaminants in the producer gas and in the engine's exhaust are regulated emissions due to their potential to harm human health and the environment. Although, combustible gases were almost entirely consumed though the combustion of producer gas in the engine, emissions of some gases like carbon monoxide as well as PM are regulated. Phase 3 US federal regulations for spark-ignited, non-road engines of this size must emit less than 610 g/kW-hr of CO. Tier 4 diesel engine emissions must have PM emissions less than 0.4 g/kW-hr. Figure 19 shows the systems' emissions on a gram per kilowatt-hour basis compared to federal emissions regulations for both PM and CO on a log scale. The system is able to meet current engine emission standards without the need for after-treatment of the exhaust gas. Emissions from the engine are well below the permissible limits for both CO and PM and the system could therefore be used safely without harm to human health or the environment. The specific emission concentrations decreased with increasing generator load which demonstrates that the total system efficiency increases with increasing electrical load.

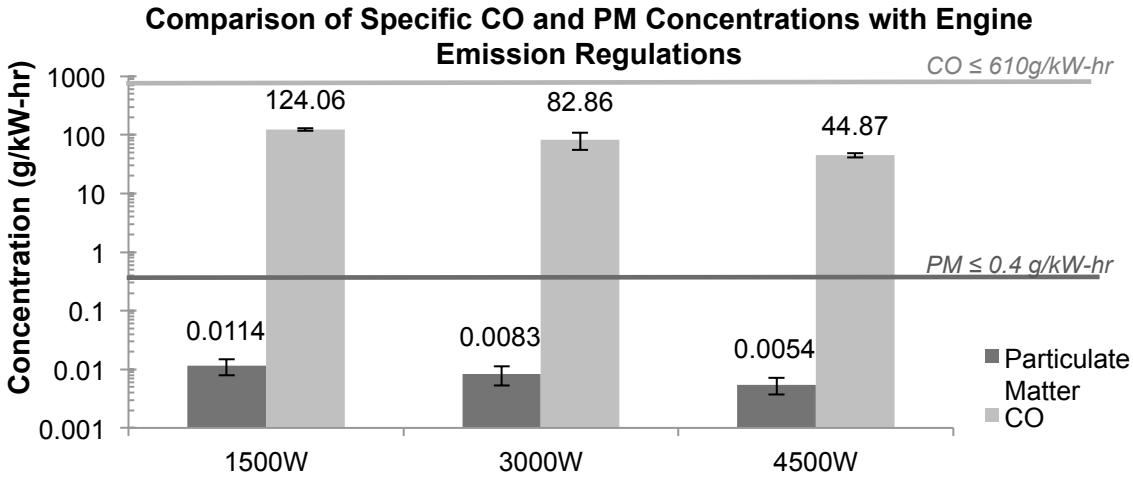


*Figure 18: Comparison of Specific CO and PM Concentrations with Engine Emission Regulations*

The elemental carbon (EC) and organic carbon (OC) concentrations were measured at the three sampling locations throughout the system at various generator loading conditions. The concentrations of total EC and total OC are shown in Figure 20. The concentrations of EC and OC were, like the gaseous compounds and particulate matter emissions, independent of generator loading. The concentrations of EC were approximately 200 $mg/m^3$, 0.3 $mg/m^3$ and 0.3 $mg/m^3$ for the pre-filtered producer gas, filtered producer gas, and engine exhaust, respectively. OC concentrations were 200 $mg/m^3$, 8 $mg/m^3$ and 7 $mg/m^3$ for the pre-filtered producer gas, filtered producer gas, and engine exhaust, respectively.

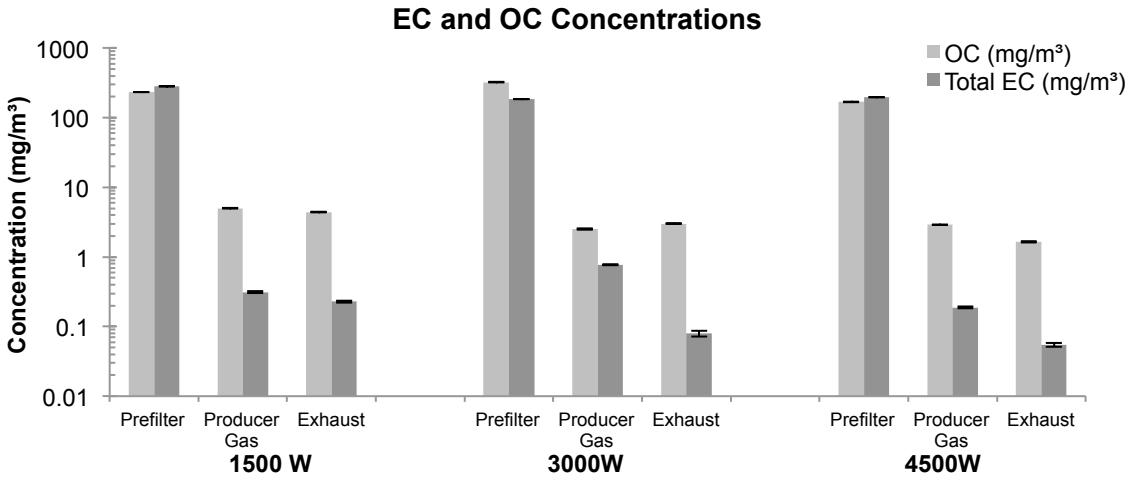


*Figure 19: EC and OC Concentrations at Various Loading Conditions*

The concentrations of OC were reduced through the packed bed filter for all loading conditions. OC was able to condense onto the material in the much cooler packed bed filter thus reducing the concentration significantly. EC concentrations were also reduced significantly through the packed bed filter. Some of the total EC content in the biomass-derived gaseous fuel leaving the reactor was removed by the PM cyclone prior to any sampling and additional EC content was removed in the packed bed filter. Both EC and OC concentrations remained stable through the engine. The engine did not change the concentrations of the PM nor did it change the OC to EC ratio of the PM. As shown in Figure 21, the ratio of OC to EC is close to one for the pre-filtered producer gas. The OC to EC ratio is significantly higher for post-filter producer gas and engine exhaust as more of the EC was removed than OC in the packed bed filter.

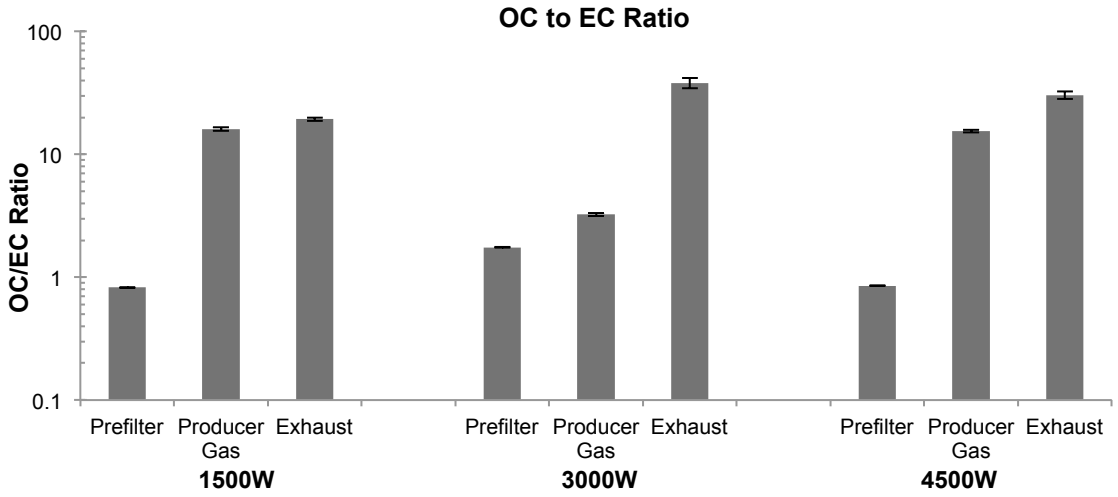


*Figure 20: OC to EC Ratio at Various Generator Loading Conditions*

### 4.2.2. Effect of Electrical Loading on Aromatic Hydrocarbon Concentrations

Biomass gasification is known to produce BTEX compounds. This study examined to what extent these harmful compounds were eliminated or reduced by the filter and engine. The concentrations of these light tars, which consist of volatile organic compounds, were generally not removed by the filter but were significantly reduced through combustion in the engine. Concentrations of BTEX compounds did not vary significantly with generator loading condition but their concentrations were reduced significantly as the biomass derived gas passed through the entire system. Among the BTEX compounds, benzene was reduced by about 96% through the engine, toluene was reduced by 75%-95% in the engine, ethylbenzene was almost entirely eliminated, and m- and p- xylenes were reduced by 48-60%.

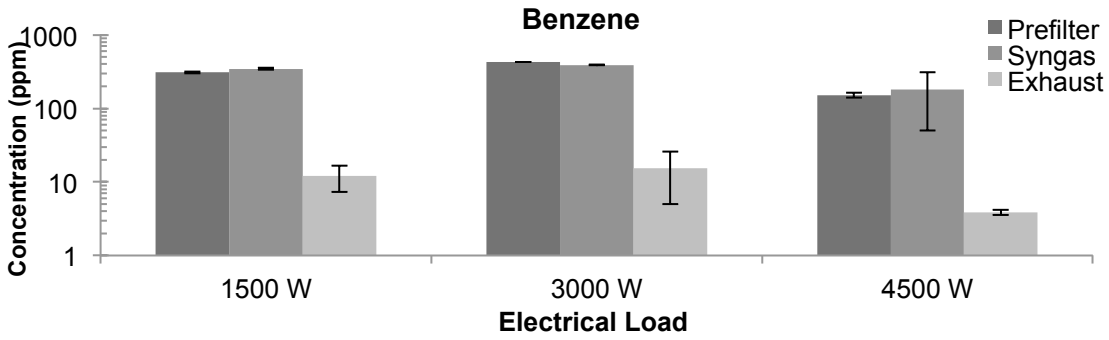


*Figure 21: Benzene Concentrations at Various Loading Condition*

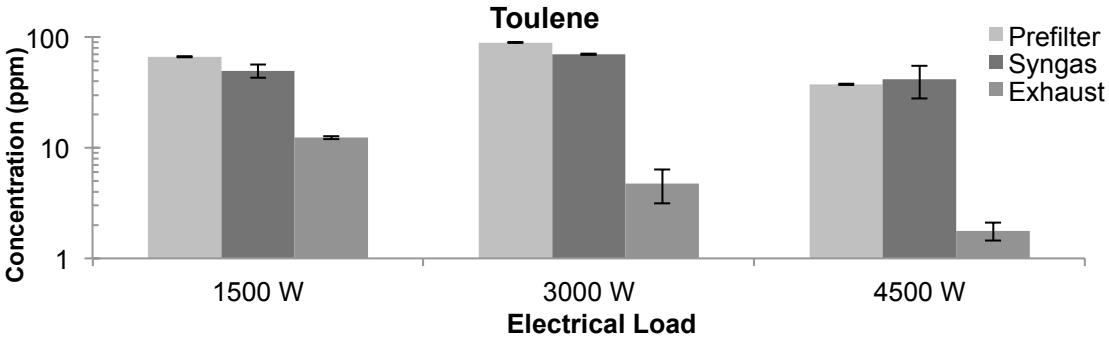


*Figure 22: Toluene Concentrations at Various Loading Conditions*

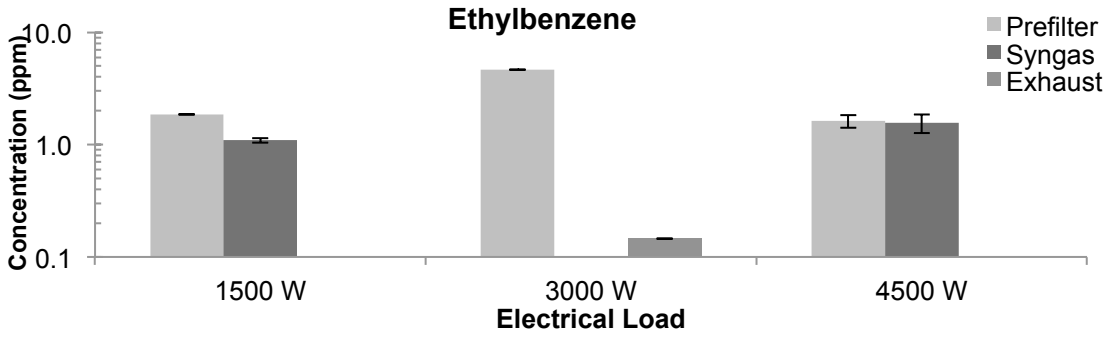


*Figure 23: Ethylbenzene Concentrations at Various Loading Conditions*

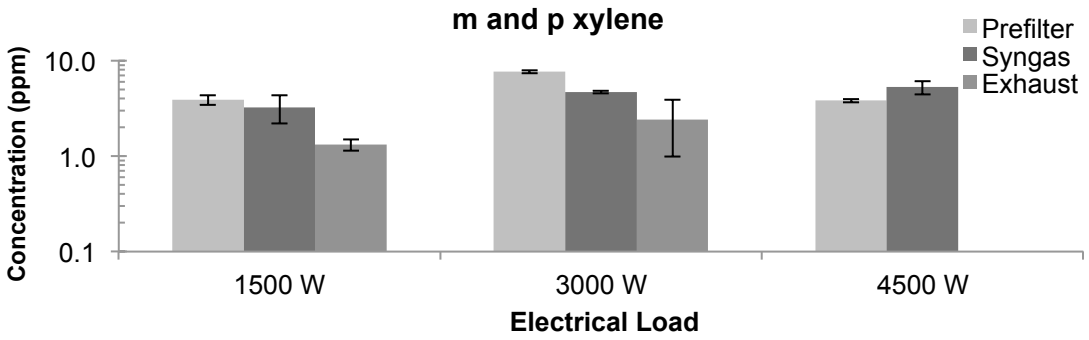


*Figure 24: m- and p- xylene Concentrations at Various Loading Conditions*

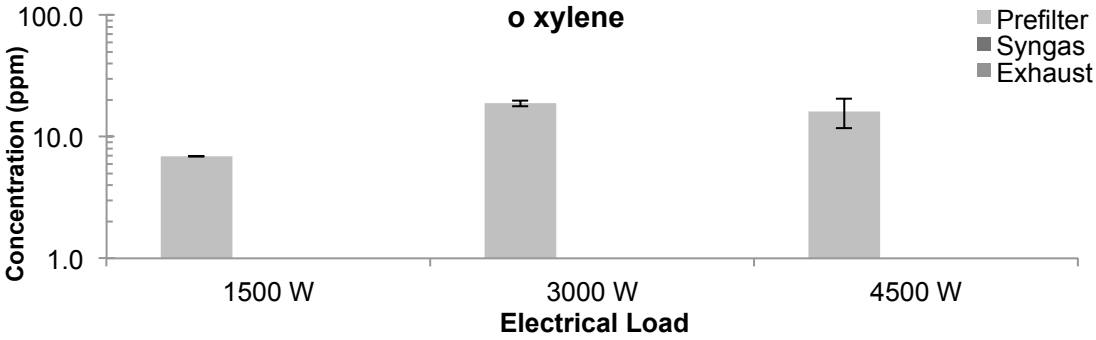


*Figure 25: o-xylene Concentrations at Various Loading Conditions*

The highest concentrations of BTEX compounds found in the system were measured for benzene followed by toluene in the pre-filtered and filtered producer gas. NIOSH recommends short term exposure limits (STEL) for benzene at 5 ppm and a time weighted average (TWA) for an eight hour work day at 1ppm. Concentrations of benzene were well above the NIOSH recommendations for unfiltered producer gas and filtered producer gas, but these gases are not being exhausted to the environment. Although the concentrations of benzene are still higher than the TWA and STEL from the engine exhaust, which is released to the environment, NIOSH recommendations are for

ambient air rather than concentrated gases. The engine's ability to reduce the concentration of all the BTEX compounds is significant. With the exception of m and p xylene which were significantly reduced, the engine is able to reduce concentrations of the hazardous VOCs to about 10ppm for many species in the exhaust gas. While these concentrations are still high, if the system is operated in a well-ventilated area, it would not pose significant risk to human health and the environment through the engine's emissions. It is possible to maintain low levels of hazardous compounds being emitted from the system by eliminating leaks from the system and ensuring that there is complete combustion in the engine.

## 5. Conclusions and Recommendations

This study quantified contaminants in producer gas generated in a 10 kW downdraft gasifier operating with woodchips, determined the engine's ability to eliminate key harmful contaminants, and performed an energy balance on the small-scale gasifier-generator system.

Concentrations of gaseous compounds, particulate matter, organic solvents, elemental carbon and organic carbon were constant as a function of generator load. As the gasifier was greatly oversized for the generator loads and engine demands tested in this study, the system was able to easily meet the changing electrical loading demands on the generator. This suggests that the process control unit and governor in the system were operating effectively to maintain stable operation over a wide range of operating conditions with the exception of the 3000 W loading condition, which showed higher than average experimental error. The efficiency of the reactor increased significantly over the range of generator loads due to the increasing throughputs of biomass into the constant temperature reactor as the heat loss from the reactor was a smaller portion of the work from the engine. As the overall efficiency of the system increased with increasing load as a result of increasing gasifier efficiency, it is beneficial to operate the system closer to its rated capacity to increase the flow rates of material through the system.

The system was able to reduce the concentrations of many of the contaminants created in the system through the use of the particle cyclone, packed bed filter, and engine. Concentrations of combustible compounds in the producer gas were consumed by 96%-98% in the engine and the concentrations of particulate matter were reduced by 98%

in the packed bed filter. PM concentrations were not changed significantly through the engine but PM emissions from the engine were still below specific federally mandated emissions limits for this type of engine without the need for after-treatment. Many BTEX compounds passed through the packed bed filter without reductions in concentration but were then reduced during the combustion in the spark-ignited engine. While the levels of these BTEX contaminants from the engine's emission are about 10 ppm each for benzene and toluene in a properly ventilated environment, the concentrations would not exceed permissible exposure limits set forth by NIOSH for ambient air. The system is able to effectively clean up many of the contaminants generated during the gasification process. A key conclusion of this work is that such small-scale gasifier-generator systems could be implemented in a rural community to efficiently utilize biomass without posing significant risk to human health and the environment.

Recommendations for future work on this project include reducing experimental error, especially in 3000W generator loading. Additionally, total hydrocarbon and NOx emissions measurements would be useful to determine if the system was able to meet all engine emissions regulations. Additionally, instrumenting the system to measure in-cylinder pressure data would allow for better understanding of the engine's operation on biomass derived gaseous fuel. Real-time particulate matter distributions would give a better understanding of PM morphology throughout the system. This would require the addition of a dilution system from engine exhaust in order to utilize a Scanning Mobility Particle Sizer (SMPS). Finally, a comparison of PM size distributions with and without a catalytic stripper would be necessary to better determine the proportions of solid and

volatile particulate matter present in the gaseous fuel and engine emissions. This could be performed either with real time size distribution scans using an SMPS or gravimetrically using a multiple stage impactor. Future work might also incorporate various feedstocks to better determine the characteristics of contaminants and emissions from different biomass types.

**References**


Ahmed, Sultan, Al Jaber, Robert Dixon, Michael Eckhart, Griffin Thompson, and David Hales. 2012. "Renewables 2012: Global Status Report 2012."

Akudo, Christopher Osita. 2008. "Quantification of Tars and Particulates from a Pilot Scale, Downdraft Biomass Gasifier". Master's thesis, Louisiana State University.

Al-Dury, Sausan Salem Kadam. 2009. "Removal of Tar in Biomass Gasification Process Using Carbon Materials." *Chemical Engineering Transactions* 18. doi:10.3303/CET0918108.

All Power Labs. 2013. "Introducing the Power Pallet."

Arvizu, D., T. Bruckner, O. Edenhofer, S. Estefen, A. Faaij, M. Fischedick, G. Hiriart, O. Hohmeyer, K. G. T. Hollands, J. Huckerby, S. Kadner, Å. Killingtveit, A. Kumar, A. Lewis, O. Lucon, P. Matschoss, L. Maurice, M. Mirza, C. Mitchell, W. Moomaw, J. Moreira, L. J. Nilsson, J. Nyboer, R. Pichs, Madruga, J. Sathaye, J. Sawin, R. Schaeffer, T. Schei, S. Schlömer, K. Seyboth, R. Sims, G. Sinden, Y. Sokona, C. von Stechow, J. Steckel, A. Verbruggen, R. Wiser, F. Yamba, T. Zwickel. 2011. In IPCC Special Report on Renewable Energy Sources and Climate Change Mitigation [O. Edenhofer, R. Pichs Madruga, Y. Sokona, K. Seyboth, P. Matschoss, S. Kadner, T. Zwickel, P. Eickemeier, G. Hansen, S. Schlömer, C. C. von Stechow (eds)], Cambridge University Press, Cambridge, United Kingdom and New York, NY, USA.

Atmospheric Recovery Inc. 2010. "Laser Gas Analysis: Process Gas Management". Eden Prairie, MN.

Bayliss, David, Chao Chen, Annie Jarabek, Babasaheb Sonawane, Lawrence Valcovic. 1998. "Carcinogenic Effects of Benzene: An Update." US Environmental Protection Agency, Washington, DC.

Belgiorno, V, G De Feo, C Della Rocca, and R M a Napoli. 2003. "Energy from Gasification of Solid Wastes." *Waste Management* 23 (1) (January): 1–15.

Biedrzycki, Stephen. 2011. "Advanced Techniques for Gas-Phase Raman Spectroscopy". University of Pittsburgh.

Birch, ME, and RA Cary. 1996. "Elemental Carbon-Based Method for Monitoring Occupational Exposures to Particulate Diesel Exhaust." *Aerosol Science and Technology* 25 (3): 221–241.

BTG (Biomass Energy Technologies). 1987. "Thermochemical Conversion of Biomass to Energy." Prepared for UNIDO, Vienna, Austria.

Buragohain, Buljit, Pinakeswar Mahanta, and Vijayanand S. Moholkar. 2010. “Biomass Gasification for Decentralized Power Generation: The Indian Perspective.” *Renewable and Sustainable Energy Reviews* 14 (1) (January): 73–92.

Cantrell, B. K., and K. L. Rubow. 1991. "Development of personal diesel aerosol sampler design and performance criteria." *Mining Engineering* 43, 232-236.

Chum, H, A Faaij, J Moreira, G Berndes, P Dhamija, H Dong, B Gabrielle, et al. 2011. “Bioenergy.” In *IPCC Special Report on Renewable Energy Sources and Climate Change Mitigation*, edited by O. Edenhofer, R. Pichs-Madruga, Y. Sokona, K. Seyboth, P. Matschoss, S. Kadner, T. Zwickel, et al., 209–332. Cambridge: Cambridge University Press.

Demirbaş, Ayhan. 2002. “Hydrogen Production from Biomass by the Gasification Process.” *Energy Sources* 24 (1) (January): 59–68.

Department of Health and Human Services. 2007. *NIOSH Pocket Guide to Chemical Hazards*. Cincinnati, OH: NIOSH Publications.

“Directive 2004/107/EC of the European Parliament and of the Council of 15 December 2004 Relating to Arsenic, Cadmium, Mercury, Nickel and Polycyclic Aromatic Hydrocarbons in Ambient Air.” 2004. *Official Journal of the European Union* L 23 (3).

“Directive 2008/50/EC of the European Parliament and of the Council of 21 May 2008 on Ambient Air Quality and Cleaner Air for Europe.” 2008. *Official Journal of the European Union* L 152 (1).

Edenhofer, Ottmar, Youba Sokona, Kristin Seyboth, Patrick Eickemeier, Patrick Matschoss, Susanne Kadner, Gerrit Hansen, and Timm Zwickel. 2011. “IPCC Special Report on Renewable Energy Sources and Climate Change Mitigation.”

Flowers, Lynn, William Boyes, Stiven Foster, Martin Gehlhaus, Karen Hogan, Allan Marcus, Peter McClure, Mark Osier, and Andrew Rooney. 2005. “Toxicological Review of Toluene”. US Enviromental Protection Agency, Washington, DC.

Fuchs, Michael, and Hermann Hofbauer. “Recommendations for Future Actions Regarding EU Legislation / Policy and Upgrading the Guideline to an International Standard”. Vienna.

Hasler, Ph, and Th Nussbaumer. 1998. “Particle Size Distribution of the Fly Ash from Biomass Combustion.” In *10th European Conference and Technology Exhibition: Biomass for Energy and Industry*, 1623–1625. Würzburg, Germany. http://www.verenum.ch/Publikationen/Particle_Size_PH_TN1998.pdf.

Hasler, Ph, and Th Nussbaumer. 1999. “Gas Cleaning for IC Engine Applications from Fixed Bed Biomass Gasification.” *Biomass and Bioenergy* 16: 385–395.

He, Fang, Weiming Yi, and Xueyuan Bai. 2006. “Investigation on Caloric Requirement of Biomass Pyrolysis Using TG–DSC Analyzer.” *Energy Conversion and Management* 47 (15-16) (September): 2461–2469.

Hinds, William C. 1999. *Aerosol Technology: Properties, Behavior, and Measurement of Airborne Particles*. New York: Wiley.

Kishore, V V V N. 2009. *Renewable Energy Engineering and Technology Principles and Practices*. *Renewable Energy Engineering and Technology Principles and Practices*. Vol. i. New Delhi: The Energy and Resources Institute (TERI).

Kittelson, David B, Megan Arnold, and Winthrop F Watts. 1999. “Review of Diesel Particulate Matter Sampling Methods”. Minneapolis, MN.

Kumar, Ajay, David D. Jones, and Milford a. Hanna. 2009. “Thermochemical Biomass Gasification: A Review of the Current Status of the Technology.” *Energies* 2 (3) (July 21): 556–581.

Kurz, Rainer, and Klaus Brun. 2001. “Degradation in Gas Turbine Systems.” *Journal of Engineering for Gas Turbines and Power (Transactions of the ASME)* 123 (1): 70–77.

Maniatis, K. 2008. “Progress in Biomass Gasification: An Overview.” *Progress in Thermochemical Biomass Conversion*: 1–31.

Milne, T A, N Abatzoglou, and R J Evans. 1998. “Biomass Gasifier ‘Tars’: Their Nature, Formation, and Conversion”. Golden.

Muradov, N, and T Veziroglu. 2008. “‘Green’ Path from Fossil-based to Hydrogen Economy: An Overview of Carbon-neutral Technologies.” *International Journal of Hydrogen Energy* 33 (23) (December): 6804–6839.

Ni, Meng, Dennis Y.C. Leung, Michael K.H. Leung, and K. Sumathy. 2006. “An Overview of Hydrogen Production from Biomass.” *Fuel Processing Technology* 87 (5) (May): 461–472.

Nielsen, T, H E Jørgensen, J C Larsen, and M Poulsen. 1996. “City Air Pollution of Polycyclic Aromatic Hydrocarbons and Other Mutagens: Occurrence, Sources and Health Effects.” *The Science of the Total Environment* 189-190 (96) (October 28): 41–49.

Pathak, B S, D V Kapatel, P R Bhoi, A M Sharma, and D K Vyas. 2007. “Design and Development of Sand Bed Filter for Upgrading Producer Gas to IC Engine Quality Fuel” 8: 15–20.

Pitman, R. M. 2006. “Wood Ash Use in Forestry - a Review of the Environmental Impacts.” *Forestry* 79 (5) (November 1): 563–588.

Prins, MJ. 2005. “Thermodynamic Analysis of Biomass Gasification and Torrefication”. PhD dissertation, Eindhoven University.

Prins, MJ, K Ptasinski, and F Janssen. 2007. “From Coal to Biomass Gasification: Comparison of Thermodynamic Efficiency.” *Energy* 32 (7) (July): 1248–1259.

Quaak, Peter, Harrie Knoef, and Hubert E Stassen. 1999. *Energy from Biomass: A review of Combustion and Gasification Technologies*. World Bank Technical Papers, No. 422. Washington, DC: World Bank.

Rabou, Luc P. L. M., Robin W. R. Zwart, Berend J. Vreugdenhil, and Lex Bos. 2009. “Tar in Biomass Producer Gas, the Energy Research Centre of The Netherlands (ECN) Experience: An Enduring Challenge.” *Energy & Fuels* 23 (12) (December 17): 6189–6198.

Rajvanshi, Anil K. 1986. “Biomass Gasification.” In *Alternative Energy in Agriculture*, edited by D Yogi Goswami, II:83–102. CRC Press.

Reed, TB, and A Das. 1988. “Downdraft Gasifier Engine Systems Handbook of Biomass”. Golden, CO.

Ruth, M., Mai, T., Newes, E., Aden, A., Warner, E., Uriarte, C; Inman, D., Simpkins, T. and Argo, A. 2013. *Projected Biomass Utilization for Fuels and Power in a Mature Market.* Transportation Energy Futures Series. U.S. Department of Energy by National Renewable Energy Laboratory, Golden, CO: 1-153.

Sethuraman, Sharan. 2010. “Performance of a Pilot Scale Biomass Gasification and Producer Gas Combustion System Using Feedstock with Controlled Nitrogen Content”. Iowa State University.

Sheth, Pratik N, and B V Babu. 2009. “Experimental Studies on Producer Gas Generation from Wood Waste in a Downdraft Biomass Gasifier.” *Bioresource Technology* 100 (12): 3127–3133. doi:10.1016/j.biortech.2009.01.024. http://dx.doi.org/10.1016/j.biortech.2009.01.024.

Ståhlberg, Pekka, Maija Lappi, Esa Kurkela, and Pekka Simell. 1998. *Sampling of Contaminants from Product Gases of Biomass Gasifiers*. Valtion teknillinen tutkimuskeskus. http://www.vtt.fi/inf/pdf/tiedotteet/1998/T1903.pdf.

Toms, Martin W, and David K Lewis. 1987. “Whole-Tree Chips : an Additional Energy Source for Oklahoma.” *Proceedings of the Oklahoma Academy of Science* 95: 89–95.

Turare, Chandrakant. 2002. “Biomass Gasification - Technology and Utilization Overview of Gasification Technology.” Artes Institute, University of Flensburg, Germany.

U.S. National Archives and Records Administration. 2004. *Code of federal regulations.* Title 40, Section 1039. Protection of Environment.

U.S. National Archives and Records Administration. 2008. *Code of federal regulations.* Title 40, Section 1054. Protection of Environment.

Wei, Lin. 2005. “Experimental Study on the Effects of Operational Parameters of a Downdraft Gasifier”. Master’s Thesis: Mississippi State University.

World Bank Group. 1998. “Thermal Power : Guidelines for New Plants.” In *Pollution Prevention and Abatement*, 413–426.

Yang, Haiping, Rong Yan, Hanping Chen, Dong Ho Lee, and Chuguang Zheng. 2007. “Characteristics of Hemicellulose, Cellulose and Lignin Pyrolysis.” *Fuel* 86 (12-13) (August): 1781–1788.

Zainal, Z A, R Ali, C H Lean, and K N Seetharamu. 2001. “Prediction of Performance of a Downdraft Gasifier Using Equilibrium Modeling for Different Biomass Materials.” *Energy Conversion and Management* 42: 1499–1515.

Zwart, RWR, A Bos, and J Kuipers. “Principle of OLGA Tar Removal System”. Petten, The Netherlands. www.olgatechnology.com.

**Appendix A: Matlab Gasifier Analysis**

The following Matlab code was used to process files from the Ramen Laser Gas Analyzer as well from the LabVIEW software which recorded temperatures, pressures, currents, flows, and conditions within the gasifier system. The program aligns the two data sets and computes the representative averages of the data for each sampling location and loading condition. While sampling times were significantly longer, the representative time was set to be 5 minutes in the center of each 20 minute sample. The program averages the data points over that small sample time and determines the standard deviation of the data points. The program plots time graphs of all the sampling tests and average values for the data points of interest. Finally, the program computes efficiency of the system by first calculating essential flows, molecular weight of the gas, and lower heating value.

```
format compact
clc
filename = 'Rlga_2013_07_16.xlsx';

%Input starting row of code and ending row
StartRow=66;
EndRow=3621;

%Input number of conditions tested
n=2;
conditions_tested={'S 1500kW', 'S 1500kW'};
plot_n=2;

%Start test 1
x(1)=950;
y(1)=1439;
%Start test 2
x(2)=2705;
y(2)=3052;
```

```
%Eliminate information at the front end and back end of the data which
will not be plotted
start_plot=1;
end_plot=2990;

%PowerPallet Processing%
PPfilename='PowerPallet_July_16_2013.xlsx';

%Input starting row of code and ending row
PPStartRow=368;
PPEndRow=10000;

%Input rows for each condition tested
%Start 1
PP_start(1)=876;
PP_end(1)=1167;
%Start 2
PP_start(2)=5252;
PP_end(2)=5700;

%Start PP data at the actual testing start
PPstart_important=1;
PPend_important=6000;

%%%%%%%%%%%%%%%%%%%%%%%%%%%%%%%%%%%%%%%%%%%%%%%%%%%%%%%%%%%%%%%%%%%%%%%%%%%%

starts=x-StartRow;
ends=y-StartRow;

%Converts to strings and concatenates
SRow=num2str(StartRow);
ERow=num2str(EndRow);
ColumnStart='D';
Colon=':';
ColumnEnd='AK';
xlRange=strcat(ColumnStart, SRow, Colon, ColumnEnd, ERow);
sheet=1;

%Imports data from Excel file into Matlab
RLGAData = xlsread(filename, sheet, xlRange);

%Time
time=5; %(minutes) length of time for intervals of sampling for
statistical purposes
length=1; %(seconds) length of time between data measurements

%Make row vector of all headers from excel file
Headers={'CO', 'H2O', 'NO2', 'O2', 'H2', 'CO2', 'N2', 'CxHy', 'x', 'x',
'x', 'x', 'x', 'x', 'x', 'Ar', 'Total 1-8', 'Total 1-16', 'Mode', 'Mode
Time', 'Warn-Low', 'Warn-High', 'Fault-Low', 'Fault-High', 'Laser, vdc',
'Laser %', 'Cell,mmHg', 'Cell, defF', 'Prism, degF,', 'Pump Area, degF',
```

```
'Remote, degF', 'Air Intake, degF', 'Flow Rate mm/min', 'Atm Pressure,
mmHg'};

%Checks size of matrices
sD=size(RLGAData);
sH=size(Headers);

if sD(2)==sH(2)
    s=sD(2);
%Computes the middle time minutes based on the starting and ending
times ofeach condition tested.

    time=5; %(minutes) length of time for intervals of sampling for
statistical purposes
    length=1; %(seconds) length of time between data measurements
    number_lines=time*60/length;

    number_rows=zeros(1,8);
    center=zeros(1,8);
    central_start=zeros(1,8);
    central_end=zeros(1,8);

for k=1:n
        number_rows(k)=ends(k)-starts(k)+1;
        center(k)=starts(k)+floor(number_rows(k)/2);
        central_start(k)=center(k)-number_lines/2;
        central_end(k)=center(k)+number_lines/2;
end

    minimums=zeros(1,s);
    maximums=zeros(1,s);
for count=1:s
        minimums(1,count)=min(RLGAData(:,count));
        maximums(1,count)=max(RLGAData(:,count));
if minimums(1, count)==maximums(1, count)
            minimums(1, count)=minimums(1, count)-1;
            maximums(1, count)=maximums(1, count)+1;
end
end

    Y_limits=[minimums', maximums'];

    Xstarts=zeros(8,2);
    Xends=zeros(8,2);
    Xcentral_s=zeros(8,2);
    Xcentral_e=zeros(8,2);

for times=1:n
        Xstarts(times,:)=[starts(times) starts(times)]-start_plot;
        Xends(times,:)=[ends(times) ends(times)]-start_plot;
```

```
        Xcentral_s(times,:)=[central_start(times)
central_start(times)]-start_plot;
        Xcentral_e(times,:)=[central_end(times) central_end(times)]-
start_plot;
end

    labels=cell(8,1);
    Xmarks=sort(starts-start_plot);
for h=1:s
if h>=1 && h<=8
if h==1
                figure
end
            hold on
            subplot(4,2,h)
            plot(RLGAData(start_plot:end_plot,h))
            set(gca,'Ylim',[minimums(h) maximums(h)],'XTick', Xmarks ,
'tickdir', 'out', 'xticklabel', conditions_tested)
            title_header=Headers(1,h);
            title(Headers(1,h))
            labels(h,:)=strcat('% ',' ', Headers(:,h));
            hold on
for t=1:n
                plot(Xstarts(t,:),Y_limits(h,:),'g')
                plot(Xends(t,:),Y_limits(h,:),'r')
                plot(Xcentral_s(t,:),Y_limits(h,:),'k')
                plot(Xcentral_e(t,:),Y_limits(h,:),'k')
end
            ylabel(labels(h,:))
end
        hold off
end


    Average=zeros(n, s);
    Error=zeros(n,s);
for ind=1:n;
if ind==1;
            RLGA1=RLGAData(central_start(ind):central_end(ind),1:s);
            Average(ind,:)=mean(RLGA1);
            Error(ind,:)=std(RLGA1);
elseif ind==2
            RLGA2=RLGAData(central_start(ind):central_end(ind),1:s);
            Average(ind,:)=mean(RLGA2);
            Error(ind,:)=std(RLGA2);
elseif ind==3
            RLGA3=RLGAData(central_start(ind):central_end(ind),1:s);
            Average(ind,:)=mean(RLGA3);
            Error(ind,:)=std(RLGA3);
elseif ind==4
            RLGA4=RLGAData(central_start(ind):central_end(ind),1:s);
            Average(ind,:)=mean(RLGA4);
```

```
            Error(ind,:)=std(RLGA4);
elseif ind==5
            RLGA5=RLGAData(central_start(ind):central_end(ind),1:s);
            Average(ind,:)=mean(RLGA5);
            Error(ind,:)=std(RLGA5);
elseif ind==6
            RLGA6=RLGAData(central_start(ind):central_end(ind),1:s);
            Average(ind,:)=mean(RLGA6);
            Error(ind,:)=std(RLGA6);
elseif ind==7
            RLGA7=RLGAData(central_start(ind):central_end(ind),1:s);
            Average(ind,:)=mean(RLGA7);
            Error(ind,:)=std(RLGA7);
else
            RLGA8=RLGAData(central_start(ind):central_end(ind),1:s);
            Average(ind,:)=mean(RLGA8);
            Error(ind,:)=std(RLGA8);
end
end

for col=1:sH(2)
if col>=1 && col<=8
if col==1
                figure
end
            subplot(5,2,col)
            errorbar(Average(1:plot_n,col), Error(1:plot_n,col),'x')
            title(Headers(1,col))
            set(gca, 'XTick', 1:plot_n, 'XTickLabel',
conditions_tested(1:plot_n));
elseif col==16
            subplot(5,2,9:10)
            errorbar(Average(1:plot_n,col), Error(1:plot_n,col),'x')
            title(Headers(1,col))
            set(gca, 'XTick', 1:plot_n, 'XTickLabel',
conditions_tested(1:plot_n));
end
end

end

Average_mixed_units=Average(:,1:8);
Average_mixed_units(:,3)=Average_mixed_units(:,3)*10000;
units(1:9)={'Percent'};units(1,3)={'ppm'};
sum_rows=(sum(Average(:,1:8)'))';
Composition=['Load and Gas', Headers(:,1:8), 'Total'; 'Units', units;
conditions_tested', num2cell(Average_mixed_units(:,1:8)),
num2cell(sum_rows)]

%Headings
PPHeadings={'T_tred','T_bred','T_Filter','T Engine Exhaust','T Exhaust
Heat Exchanger In','T Exhaust Heat Exchanger Out','T Syngas Heat
```

```
Exchanger Out','T Syngas Heat Exhanger In','T Engine Intake','P Bottom
of Reactor','P Filter','P Engine Intake','DP Syngas','P Combutstion','P
Reactor Intake','O2 Sensor Raw','Fuel Switch Raw','Key Postion','Oil
Pressure','Orifice flow Kg/sec','Load Current','Air intake Reactor
Kg/sec','Air Intake Engine
kg/sec','Grate','P_ratio_reactor','P_ratio_state_reactor','Grate_Val','
P_ratio_filter','P_ratio_filter_state','Lambda_In','Lambda_Out','Lambda
_Setpoint','Lambda_P','Lambda_I','Lambda_D','FuelSwitchLevel','P_reacto
rLevel','T_tredLevel','T_bredLevel','Engine','Engine Coolant
Out','Engine Coolant In','ANA0','ANA1','ANA2','ANA3','ANA4','ANA5','
ANA6',' ANA7'};

%Converts to strings and concatenates
PPSRow=num2str(PPStartRow);
PPERow=num2str(PPEndRow);
PPColumnStart='C';
PPColumnEnd='AZ';
PPxlRange=strcat(PPColumnStart, PPSRow, Colon, PPColumnEnd, PPERow);
PPsheet=1;

%Import data to Matlab
PowerPallet=xlsread(PPfilename, PPsheet, PPxlRange);
PowerPallet(isnan(PowerPallet))=0;

PP_size=size(PowerPallet);
p=PP_size(1,2);

PP_number_rows=zeros(1,8);
PP_center=zeros(1,8);
PP_central_start=zeros(1,8);
PP_central_end=zeros(1,8);

for ppk=1:n
    PP_number_rows(ppk)=PP_end(ppk)-PP_start(ppk)+1;
    PP_center(ppk)=PP_start(ppk)+floor(PP_number_rows(ppk)/2);
    PP_central_start(ppk)=PP_center(ppk)-number_lines/2-PPStartRow;
    PP_central_end(ppk)=PP_center(ppk)+number_lines/2-PPStartRow;
end

PP_minimums=zeros(1,p);
PP_maximums=zeros(1,p);

for ppcount=1:p
    PP_minimums(1,ppcount)=min(PowerPallet(:,ppcount));
    PP_maximums(1,ppcount)=max(PowerPallet(:,ppcount));
if PP_minimums(1, ppcount)==PP_maximums(1, ppcount)
        PP_minimums(1, ppcount)=PP_minimums(1, ppcount)-1;
        PP_maximums(1, ppcount)=PP_maximums(1, ppcount)+1;
end
end
```

```
PP_Y_limits=[PP_minimums', PP_maximums'];

for tim=1:n
        PPXstarts(tim,:)=[PP_start(tim) PP_start(tim)]-
PPstart_important-PPStartRow;
        PPXends(tim,:)=[PP_end(tim) PP_end(tim)]-PPstart_important-
PPStartRow;
        PPXcentral_s(tim,:)=[PP_central_start(tim)
PP_central_start(tim)]-PPstart_important;
        PPXcentral_e(tim,:)=[PP_central_end(tim) PP_central_end(tim)]-
PPstart_important;
end

PP_labels=cell(3,1);
PPXmarks=sort(PP_start-PPstart_important-PPStartRow);
h=1;

for e=[20 22 23]
if e==20
        figure
end
    hold on
    subplot(3,1,h)
    plot(PowerPallet(PPstart_important:PPend_important,e))
    set(gca,'XLim',[0 PPend_important-
PPstart_important],'Ylim',[PP_minimums(e) PP_maximums(e)],'XTick',
PPXmarks ,'tickdir','out', 'xticklabel', conditions_tested)
    title_header=PPHeadings(1,e);
    title(PPHeadings(1,e))
    labels(e,:)=strcat('% ',' ', PPHeadings(1,e));
    hold on
for t=1:n
        plot(PPXstarts(t,:),PP_Y_limits(e,:),'g')
        plot(PPXends(t,:),PP_Y_limits(e,:),'r')
        plot(PPXcentral_s(t,:),PP_Y_limits(e,:),'k')
        plot(PPXcentral_e(t,:),PP_Y_limits(e,:),'k')
end
    ylabel(labels(e,:))
    h=h+1;
end
hold off

PP_Average=zeros(n, p);
PP_Error=zeros(n,p);

for indexpp=1:n;
if indexpp==1;

PP_1=PowerPallet(PP_central_start(indexpp):PP_central_end(indexpp),1:p)
;
        PP_Average(indexpp,:)=mean(PP_1);
        PP_Error(indexpp,:)=std(PP_1);
```

```
elseif indexpp==2

PP_2=PowerPallet(PP_central_start(indexpp):PP_central_end(indexpp),1:p)
;
        PP_Average(indexpp,:)=mean(PP_2);
        PP_Error(indexpp,:)=std(PP_2);
elseif indexpp==3

PP_3=PowerPallet(PP_central_start(indexpp):PP_central_end(indexpp),1:p)
;
        PP_Average(indexpp,:)=mean(PP_3);
        PP_Error(indexpp,:)=std(PP_3);
elseif indexpp==4

PP_4=PowerPallet(PP_central_start(indexpp):PP_central_end(indexpp),1:p)
;
        PP_Average(indexpp,:)=mean(PP_4);
        PP_Error(indexpp,:)=std(PP_4);
elseif indexpp==5

PP_5=PowerPallet(PP_central_start(indexpp):PP_central_end(indexpp),1:p)
;
        PP_Average(indexpp,:)=mean(PP_5);
        PP_Error(indexpp,:)=std(PP_5);
elseif indexpp==6

PP_6=PowerPallet(PP_central_start(indexpp):PP_central_end(indexpp),1:p)
;
        PP_Average(indexpp,:)=mean(PP_6);
        PP_Error(indexpp,:)=std(PP_6);
elseif indexpp==7

PP_7=PowerPallet(PP_central_start(indexpp):PP_central_end(indexpp),1:p)
;
        PP_Average(indexpp,:)=mean(PP_7);
        PP_Error(indexpp,:)=std(PP_7);
else

PP_8=PowerPallet(PP_central_start(indexpp):PP_central_end(indexpp),1:p)
;
        PP_Average(indexpp,:)=mean(PP_8);
        PP_Error(indexpp,:)=std(PP_8);
end
end

counter=1;
for o=[20 22 23]
if o==20
        figure
end
    subplot(3,1,counter)
    errorbar(PP_Average(1:n,o), PP_Error(1:n,o),'x')
    title(PPHeadings(1,o))
```

```
    set(gca, 'XTick', 1:n, 'XTickLabel', conditions_tested(1:n));
    counter=counter+1;
end

characters=char(conditions_tested);

matches=cell(3,n);
for c=1:2
    string_to_find=characters(c,3:8);
    matches(c,1:n)=strfind(conditions_tested, string_to_find);
end

locations_matches_1=find(~cellfun(@isempty,matches(1,:)));


MolecularMass=[28.01,18.0153,46.0055,32.00,2.016,44.01,28.02,16.04]';
Each_Element_LHV_MJkG=[10.12,0,0,0,120.971,0,0,50]';
SynComp=zeros(1,8);

Average_flows=PP_Average(1:n,[20 22 23]);
Average_flow_all_tests(1,:)=mean(Average_flows([locations_matches_1],:)
);
SynComp(1,1:8)=mean(Average([locations_matches_1],1:8));

f=1;
for r=1:1
    SyngasMolecularWt_dry(f)=(SynComp(r,:)./100)*MolecularMass;
    f=f+1;
end

m_dot_Syngas=Average_flow_all_tests(:,1); %kg/s
m_dot_Engine=Average_flow_all_tests(:,2); %kg/s
m_dot_Reactor=Average_flow_all_tests(:,3); %kg/s

Comp(1:1,1:8)=SynComp./100;
for b=1:1

m_dot_dry_total(b)=.76*m_dot_Reactor(b,:)*SyngasMolecularWt_dry(b)/(Com
p(b,7)*MolecularMass(7,:));
end

LHV_syngas=zeros(1,1);

for q=1:1

LHV_syngas(q,1)=(((Comp(q,:).*MolecularMass')*Each_Element_LHV_MJkG)/Sy
ngasMolecularWt_dry(q))*1000; %kJ/kg
end

LHV_wood=18*10^3; %kj/kg
```

```
m_dot_wood=(m_dot_Syngas-m_dot_Reactor)/.9888; %kg/s accounts for 1.12%
wood content that becomes ash

m_dot_H2O=m_dot_Syngas-m_dot_dry_total';

for z=1:1

mass_fractions_wet(z,:)=Comp(z,:).*MolecularMass'*m_dot_dry_total(z)/(m
_dot_Syngas(z,1)*SyngasMolecularWt_dry(z));
end

loads_elec= [1.500]'; %kw

power_syngas=LHV_syngas.*m_dot_dry_total'; %kj/kg*kg/s=kw
power_wood=LHV_wood.*m_dot_wood; %kj/kg*kg/s=kw

efficiency_system=loads_elec./power_wood*100;
efficiency_reactor=power_syngas./power_wood*100;
efficiency_enginegenerator=(loads_elec./power_syngas)*100;

loads={'1500 W'};

efficiency=[efficiency_system efficiency_reactor
efficiency_enginegenerator]

eff_titles={'System''Reactor''Engine Generator'};

f=8;

figure
bar(efficiency)
title('Efficiencies','fontsize',f)
ylabel('% Efficiency','fontsize',f)
set(gca, 'XTick', 1:3, 'XTickLabel', eff_titles, 'ylim', [0
ceil((max(max(efficiency)))*10^(-1))/(10^(-1))],'fontsize',f)

l=1;
pos=1;
for ind=1:1
    pos=pos-2.75;
for u=1:1
        xdsys=[efficiency(u,ind)];
        xnamesys=mat2str(xdsys,l);
        text(pos,efficiency(u,ind)+1.5, 0, '\eta
=','horizontalalignment','center','fontsize',f);
        text(pos,efficiency(u,ind)+.5, 0,
xnamesys,'horizontalalignment','center','fontsize',f);
        pos=pos+1;
end
end
```

## Appendix B: Micro GC Method

### Calibration Gases:

The following calibration gases were used to calibrate the method for both columns in the Agilent 490-MicroGC.

- Scotty 14L Calibration Gas: Natural Gas Mixture

*Table 17: Natural Gas Calibration Gas*

| Component | Gas Concentration (moles) |
|---|---|
| N-butane | 3.05% |
| Carbon Dioxide | 0.990% |
| Ethane | 9.05% |
| Helium | 0.505% |
| Isobutane | 3.02% |
| Isopentane | 0.998 |
| Nitrogen | 4.95% |
| N-pentane | 1.0% |
| Propane | 6.02% |
| Methane | Balance |

- JJS Technical Services 76L Calibration Gas: BTEX Mixture

*Table 18: JJS BTEX Mixture Calibration Gas*

| Component | Gas Concentration (moles) |
|---|---|
| Benzene | 20 ppm |
| Ethylbenzene | 20 ppm |
| Toluene | 20 ppm |
| o-Xylene | 20 ppm |
| Nitrogen | Balance |

- Scotty 74L Calibration Gas: BTEX Mixture

*Table 19: Scotty BTEX Mixture Calibration Gas*

| Component | Gas Concentration (moles) |
|---|---|
| Benzene | 10.4 ppm |
| Ethylbenzene | 10.4 ppm |
| Toluene | 10.4 ppm |
| m-Xylene | 10 ppm |
| o-Xylene | 10 ppm |
| p-Xylene | 10 ppm |
| Nitrogen | Balance |

- Scotty 4L Calibration Gas: Hydrocarbon Mixture

*Table 20: Hydrocarbon Mixture Calibration Gas*

| Component | Gas Concentration (moles) |
|---|---|
| N-butane | 14.9 ppm |
| Ethane | 15.0 ppm |
| N-hexane | 15.1 ppm |
| Methane | 15.0 ppm |
| N-pentane | 15.1 ppm |
| Propane | 14.9 ppm |
| Nitrogen | Balance |

**Method Details:**

The following method was developed in order to get adequate distinction between peaks.

*Table 21: Method Details*

| Parameter | Column 1: 10m Plora-PLOT U | Column 2: 8m 5CB Sip-Sil |
|---|---|---|
| Injector Temperature | 100°C | 100°C |
| Injection Time | 150 ms | 250 ms |
| Back flush Time | 0.00 s | n/a |
| Column Temperature | 95°C | 120°C |
| Pressure Mode | Static | Static |
| Initial Pressure | 20 PSI | 23 PSI |
| Sampling Frequency | 50 Hz | 50 Hz |
| Run Time | 100 s | 140 s |
| Acquisition Delay | 0 s | 0 s |

| Parameter | Common |
|---|---|
| Stabilizing Time | 5 s |
| Sample Time | 25 s |
| Sample Line Temperature | 110°C |
| Continuous Flow | off |
| Flush Cycles | 1 cycle |

**Calibration Curves:**

The following calibration curves were used for sample analysis of organic solvents present in the gasifier system.

- Benzene (Channel 2, 8m 5CB Heated Injector)
  Average RF: 2.40783e-007 RF StDev: 2.45753e-008 RF %RSD: 10.2064
  Scaling: None LSQ Weighting: None Force Through Zero: On
  Replicate Mode: Replace
  Fit Type: Linear y = 2.35773e-007x + 0.000000
  Goodness of fit (r^2): 0.901486

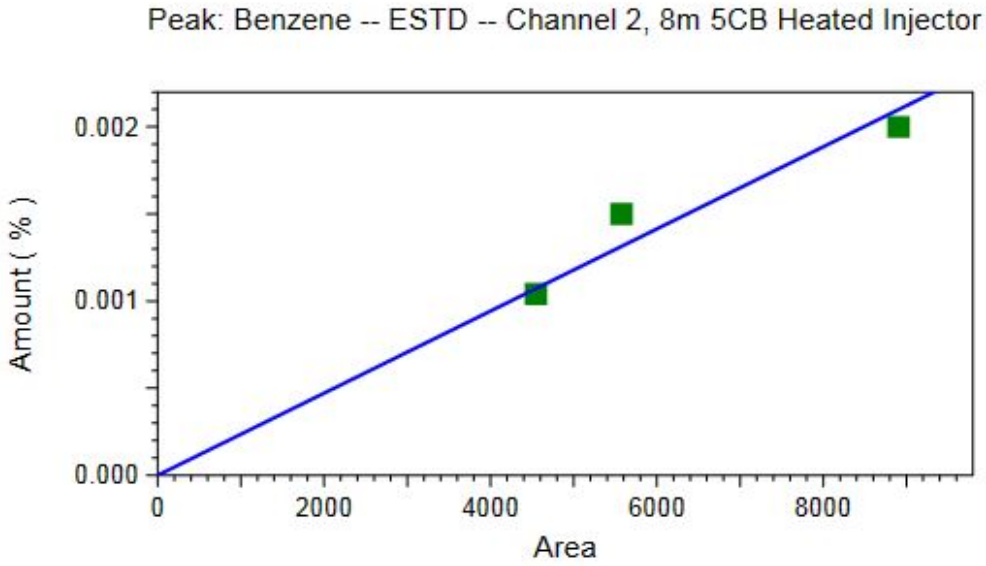


*Figure 26: Benzene Calibration Curve*

- Toluene (Channel 2, 8m 5CB Heated Injector)
  Average RF: 2.34092e-007 RF StDev: 2.79151e-008 RF %RSD: 11.9249
  Scaling: None LSQ Weighting: None Force Through Zero: On
  Replicate Mode: Replace
  Fit Type: Linear y = 2.25794e-007x + 0.000000
  Goodness of fit (r^2): 0.853315

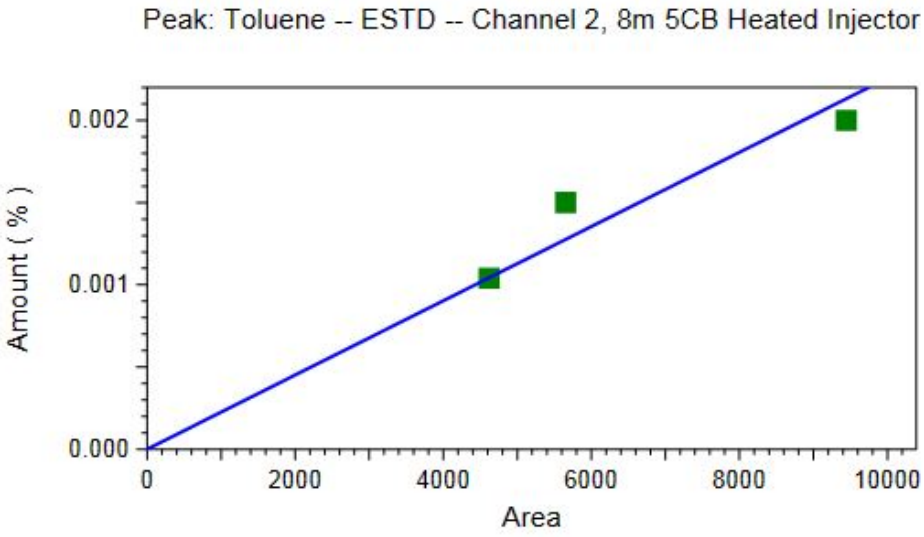


*Figure 27: Toluene Calibration Curve*

- Ethylbenzene (Channel 2, 8m 5CB Heated Injector)
  Average RF: 2.97594e-007 RF StDev: 1.71307e-008 RF %RSD: 5.75640
  Scaling: None LSQ Weighting: None Force Through Zero: On
  Replicate Mode: Replace
  Fit Type: Linear y = 3.02692e-007x + 0.000000
  Goodness of fit (r^2): 0.963204

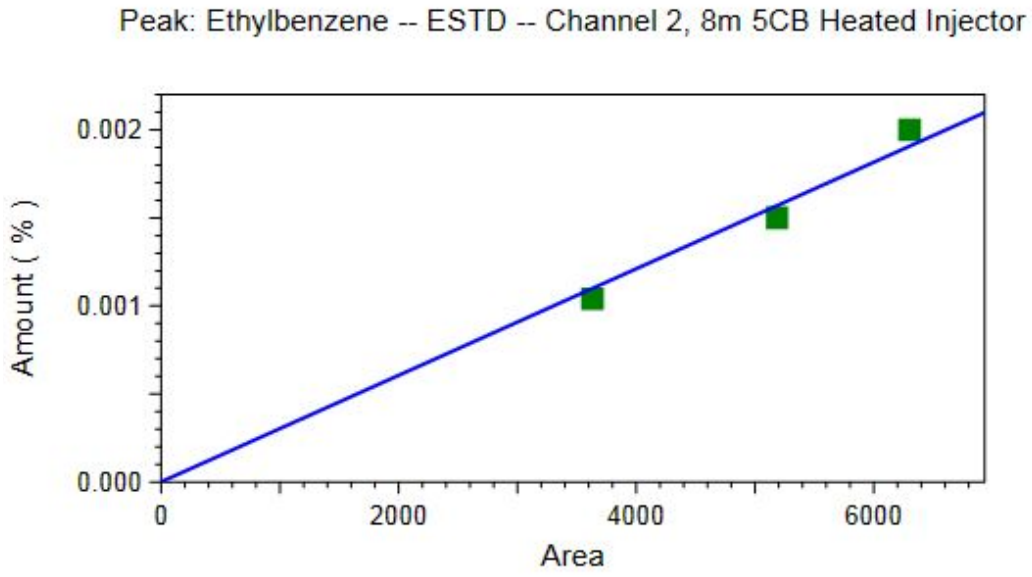


*Figure 28: Ethylbenzene Calibration Curve*

- p and m xylene (Channel 2, 8m 5CB Heated Injector)
  Average RF: 2.16380e-007
  Scaling: None LSQ Weighting: None Force Through Zero: Off
  Replicate Mode: Replace
  Fit Type: Point-to-Point

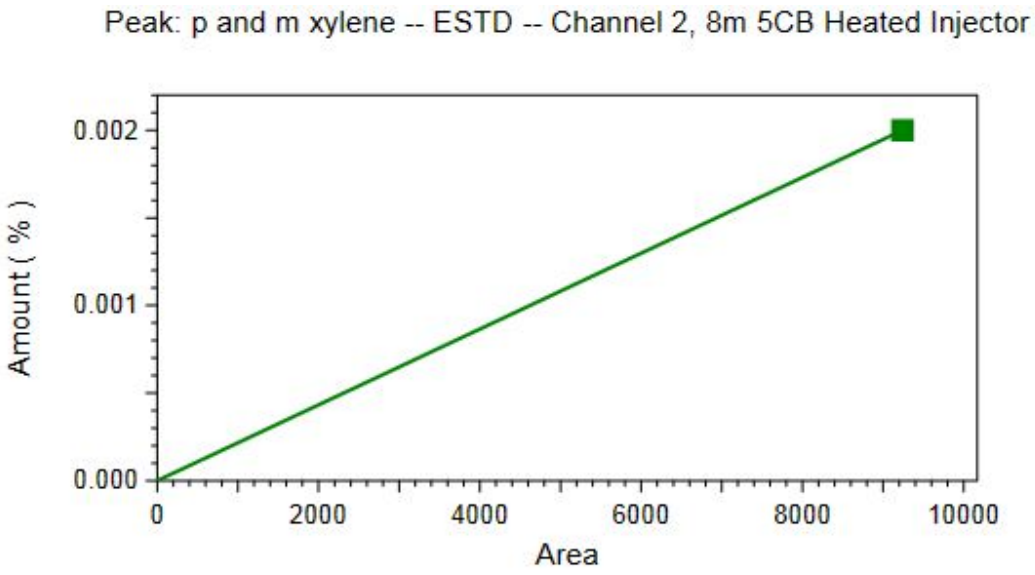


*Figure 29: p and m Xylene Calibration Curve*

- o-xylene (Channel 2, 8m 5CB Heated Injector)
  Average RF: 2.69847e-007 RF StDev: 5.47143e-008 RF %RSD: 20.2761
  Scaling: None LSQ Weighting: None Force Through Zero: On
  Replicate Mode: Replace
  Fit Type: Linear y = 2.67363e-007x + 0.000000
  Goodness of fit (r^2): 0.747256

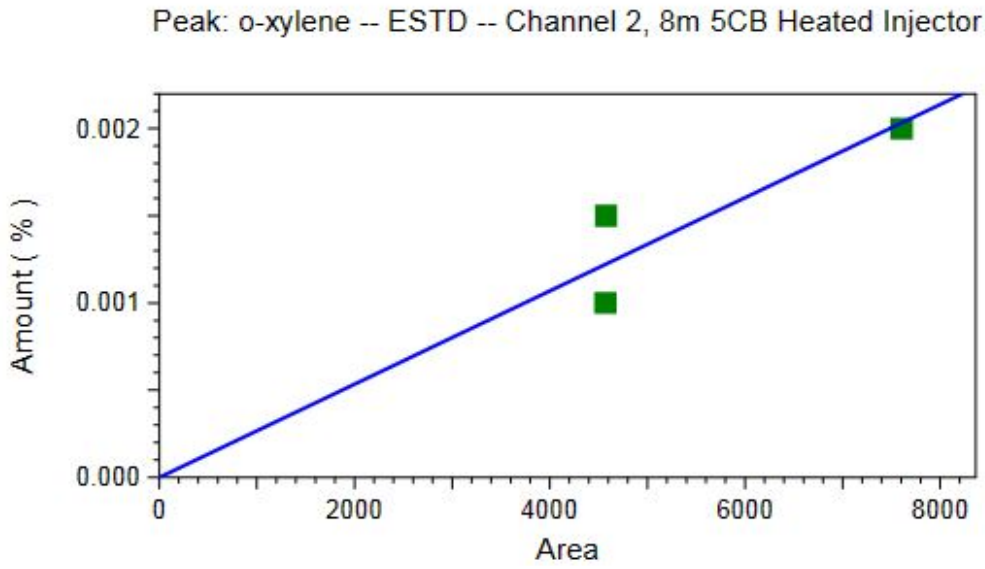


*Figure 30: o-Xylene Calibration Curve*